Severe slugging: modeling, simulation and stability criteria

Jorge Luis Baliño
jlbalino@usp.br
Departamento de Engenharia Mecânica
Escola Politécnica

Jornadas em Escoamentos Multifásicos

Universidade de São Paulo
Brasil

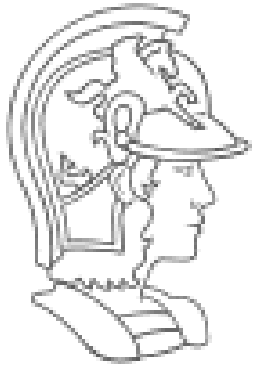

Outline

- Introduction
- Air-water model
- Simulation results
- Linear stability analysis

Some information

- Petroleum production in Brazil (2013): 985.5 million barrels of petroleum and other liquids (730 million barrels was crude oil, and 192.4 million barrels was biofuels) and 25.8 billions of cubic meters of natural gas.
- More than 91% of Brazil's oil production is offshore in very deep water and consists of mostly heavy grades, of which 79% was developed near the state of Rio de Janeiro, primarily in the Santos and Campos basins.
- Pre-salt (1000-2000 m water layer, 4000-6000 m under seabed) accounts for 15% of total oil production. Estimated pre-salt reserves: over 50 billion barrels of oil.
- Transported fluid is a multiphase, multicomponent mixture of oil, gas and water.
- Possible formation of emulsions, hydrates and wax.
- Modeling and simulation is very complex (flow assurance).

Offshore petroleum production systems

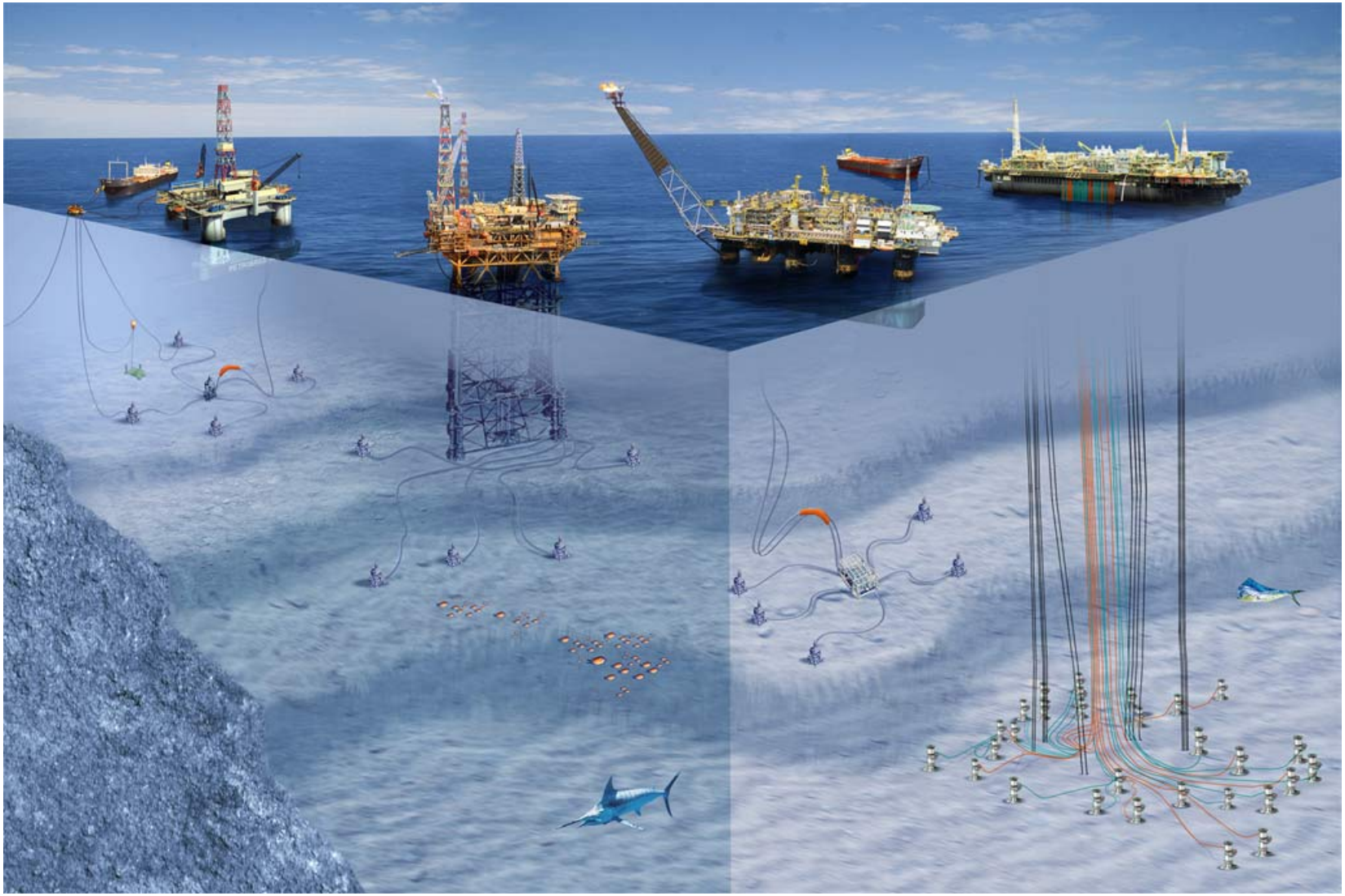

Offshore petroleum production systems

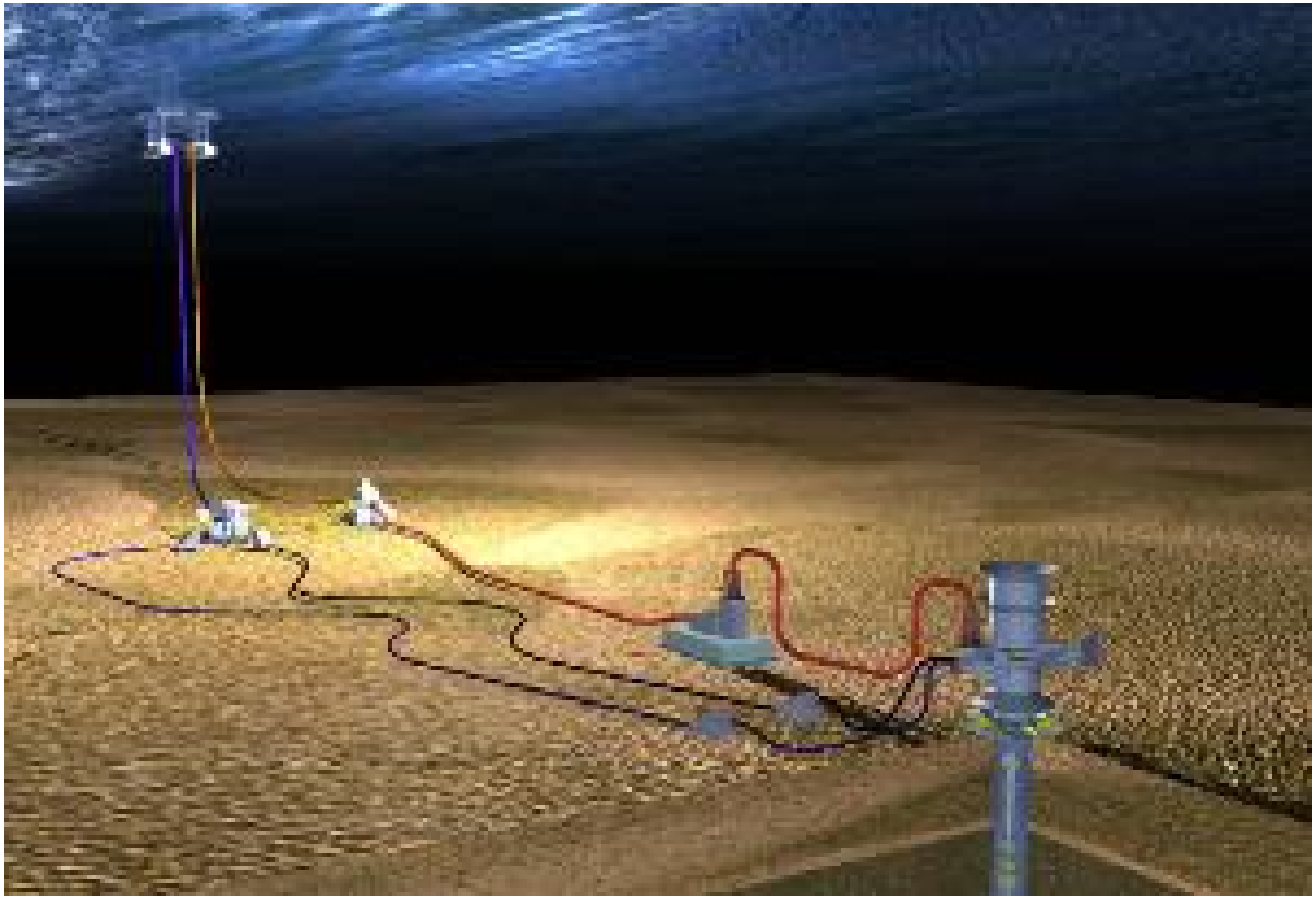

Motivation

- 2005: First contract between USP and Petrobras in the area of severe slugging in catenary risers.
- Analysis of experimental results in an air-water rig, made by CALTec (UK) under request of Petrobras, related to the influence of separator pressure in catenary riser (Wordsworth *et al*., 1998).
- Three main areas: modeling and simulation, stability analysis and multiphase rig.

Stationary state

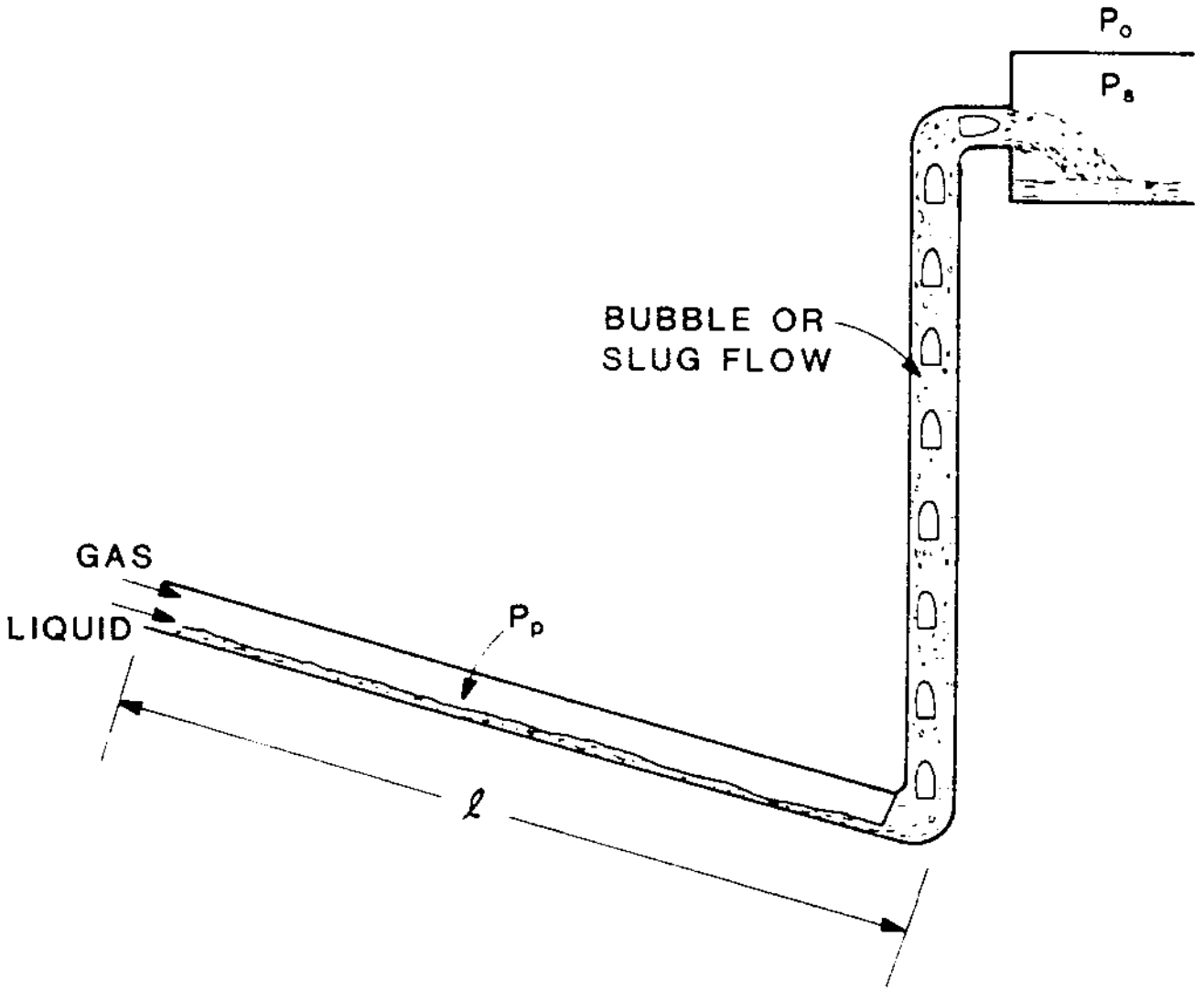

Taitel (1986)

Slug formation

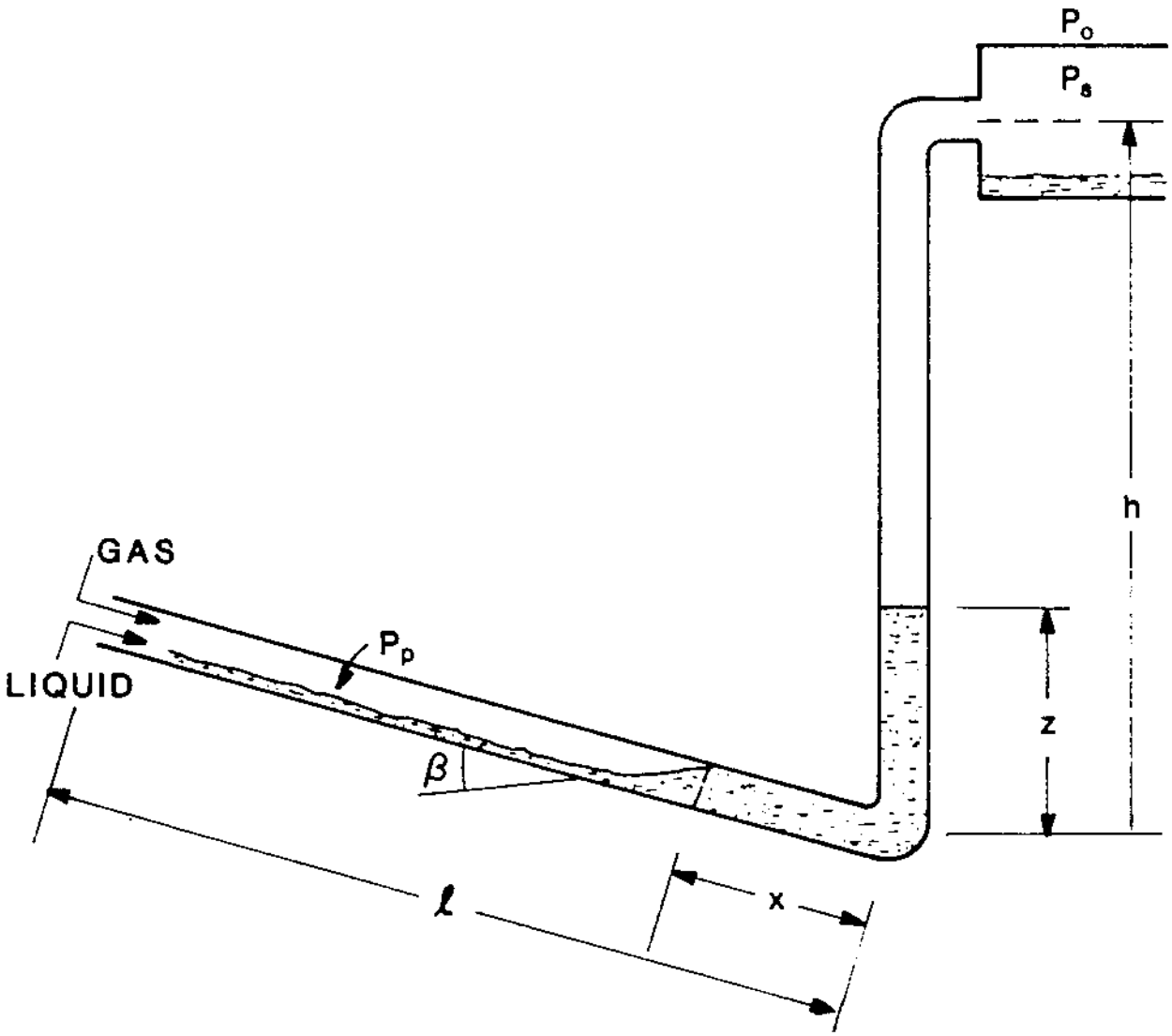

Taitel (1986)

Slug production

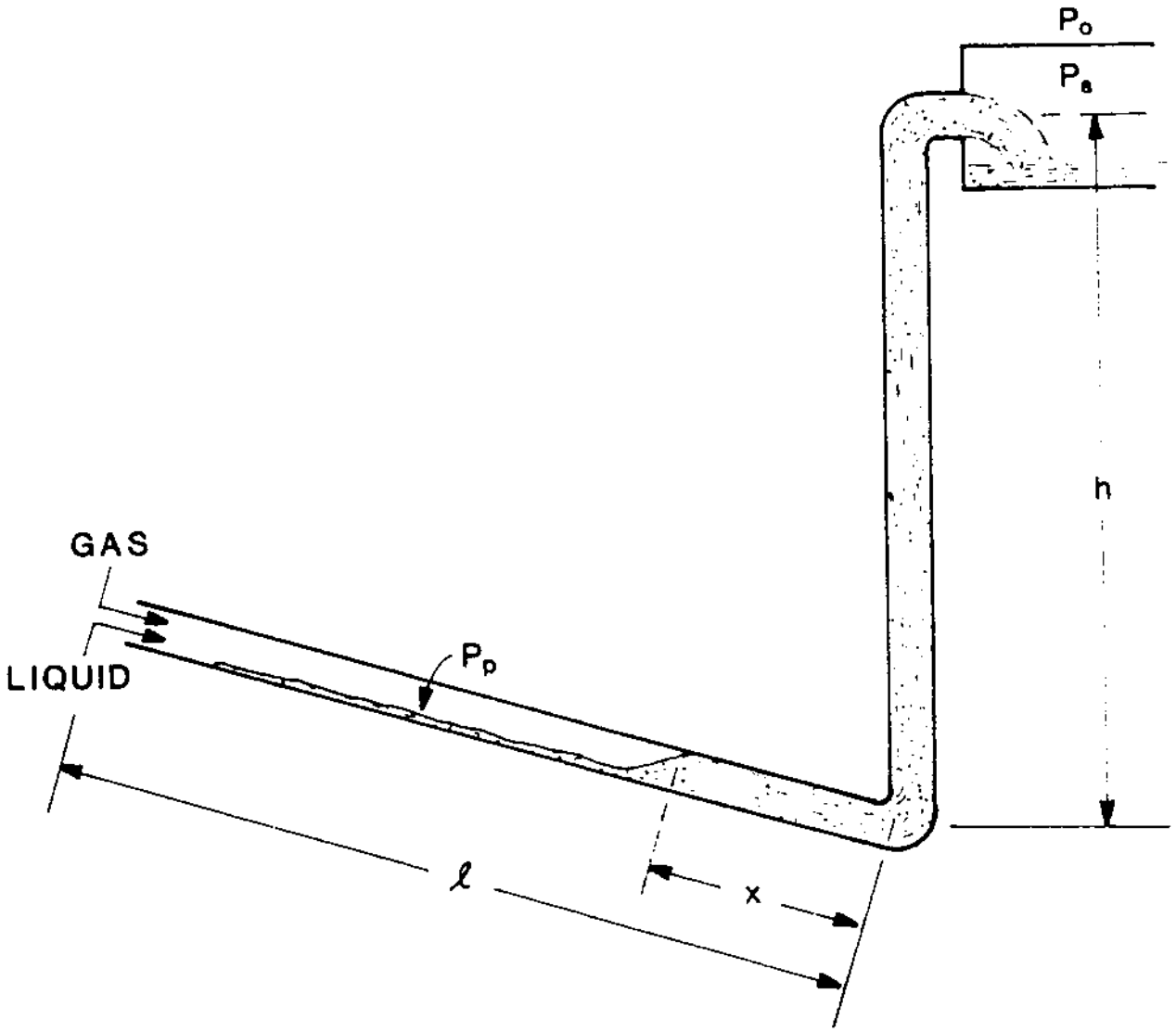

Taitel (1986)

Blowout

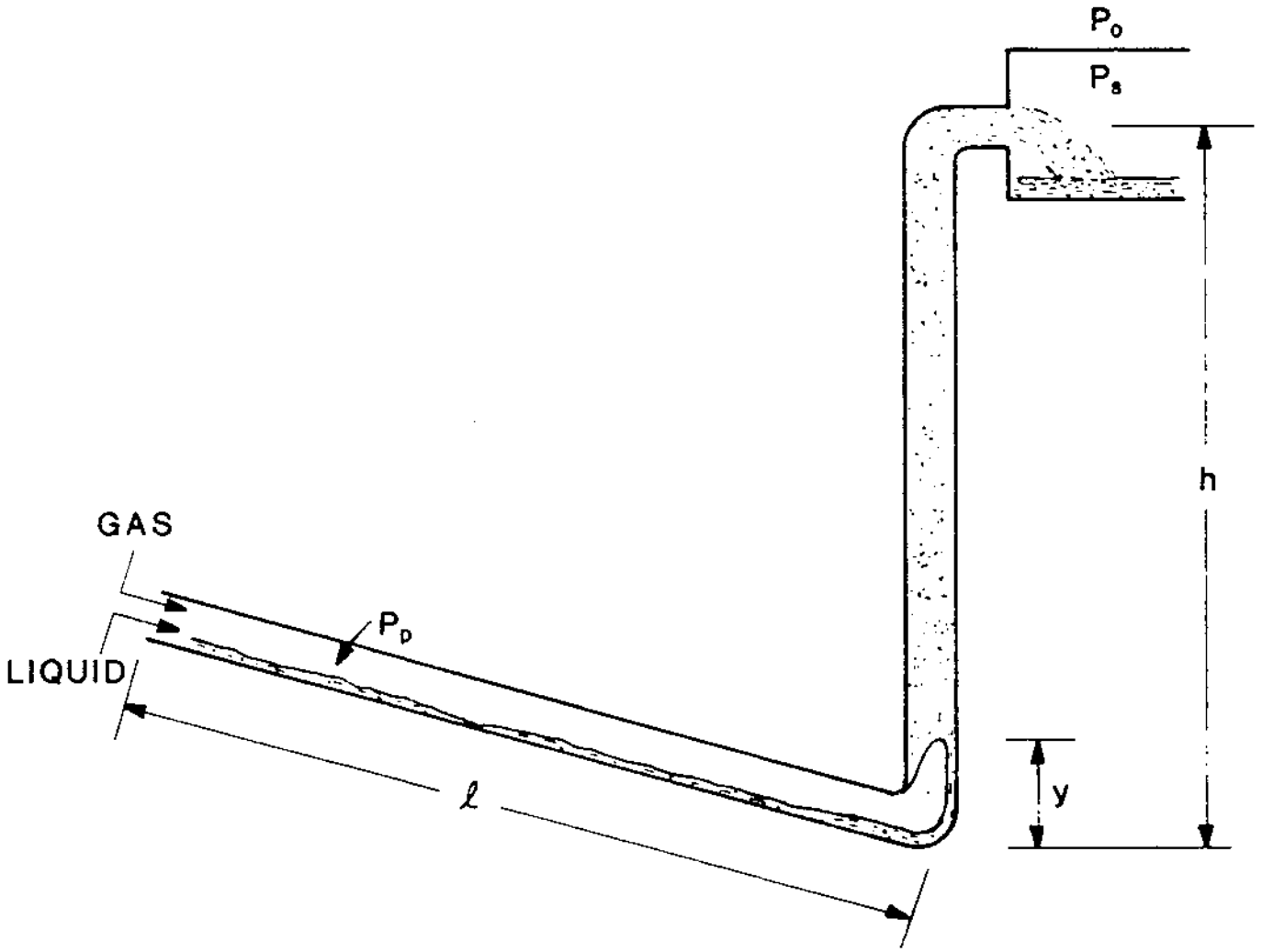

Taitel (1986)

Blowdown

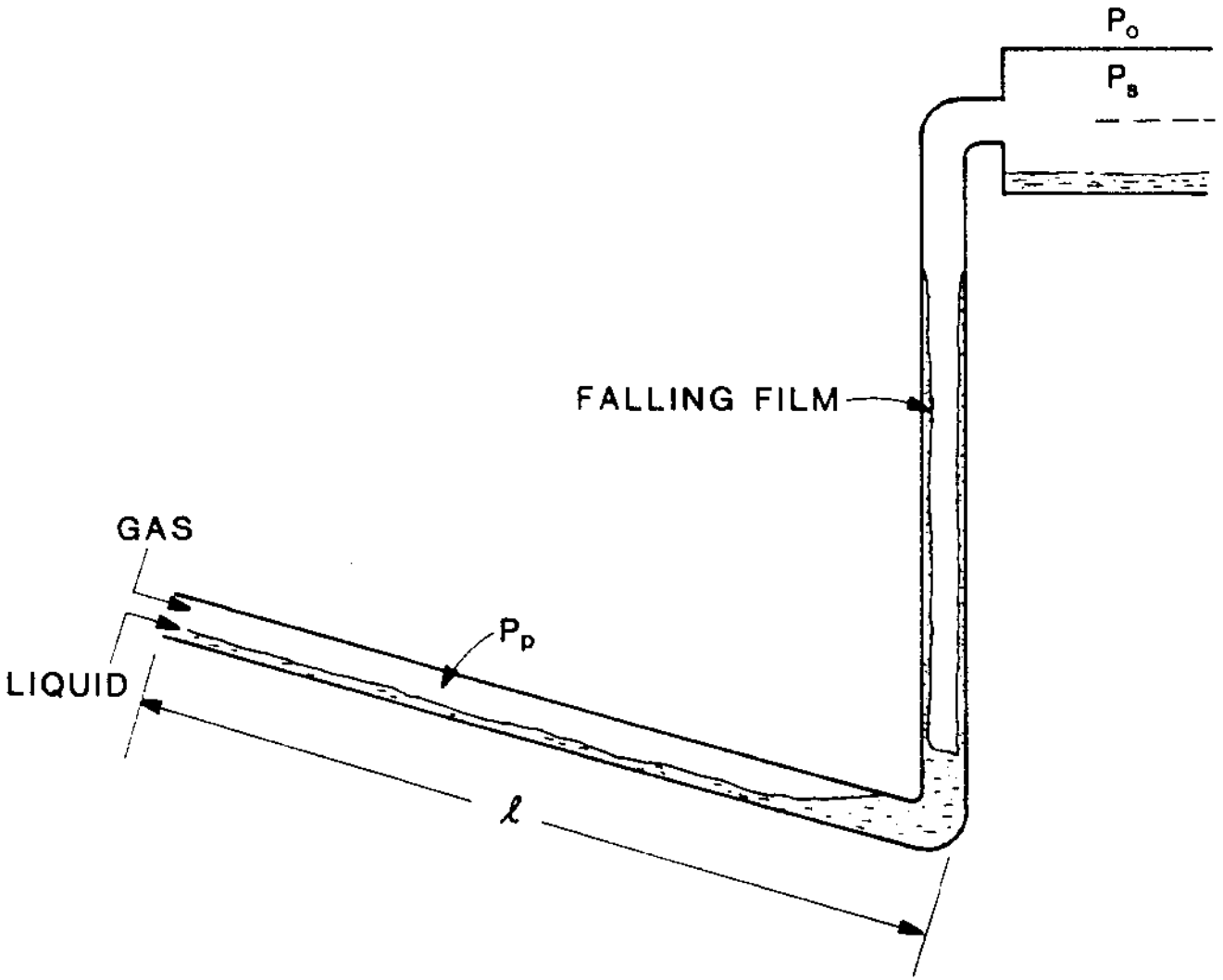

Taitel (1986)

Severe slugging cycle

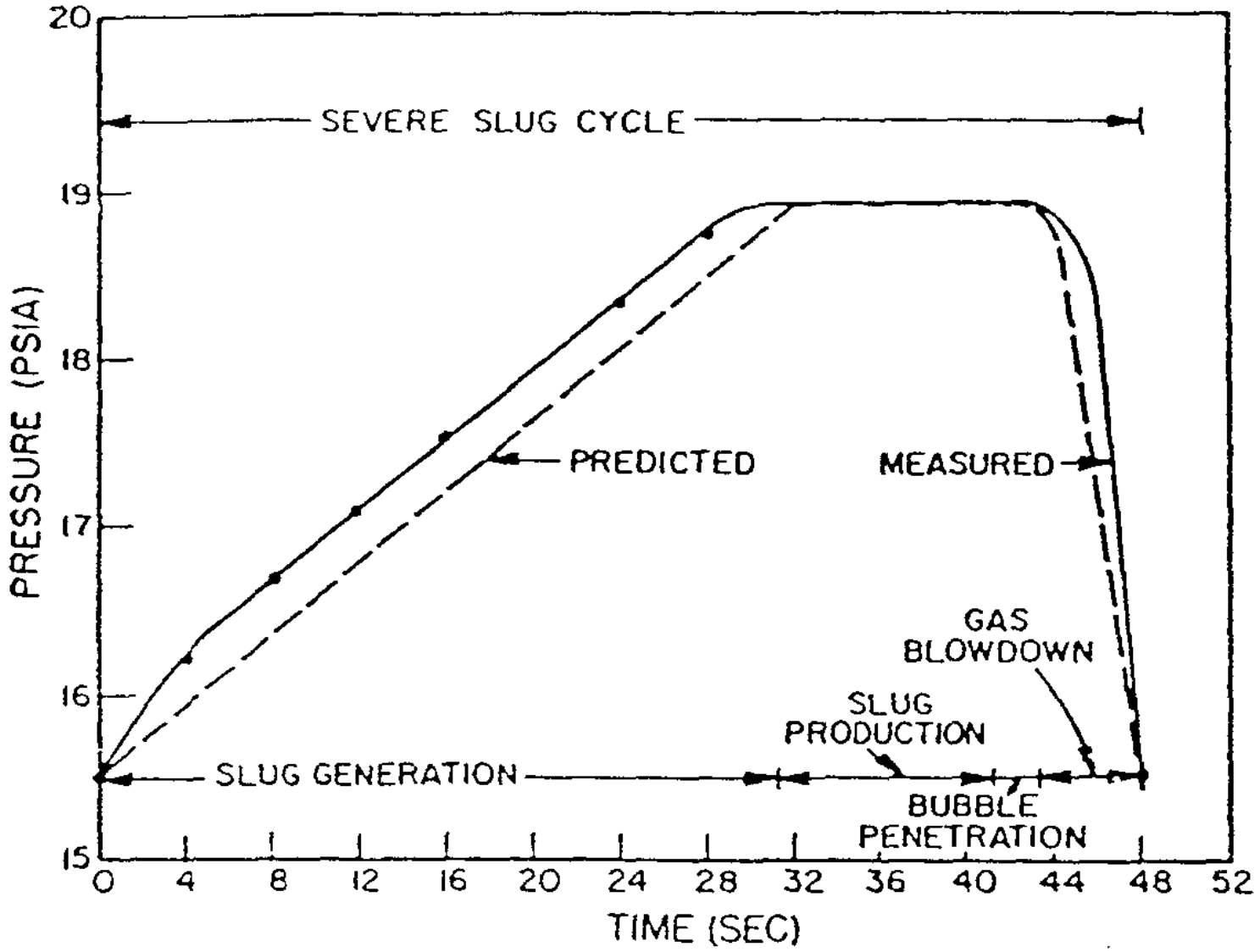

Schmidt (1977)

S n)

Severe slugging

- Terrain dominated phenomenon, characterized by the formation and cyclical production of long liquid slugs and fast gas blowdown.
- Instability that may may appear for low gas and liquid flow rates.
- Main issues related to severe slugging are:
  - High average back pressure at well head, causing tremendous production losses.
  - High instantaneous flow rates, causing instabilities in the liquid control system of the separators and eventually shutdown.
  - Reservoir flow oscillations.

Severe slugging cycle

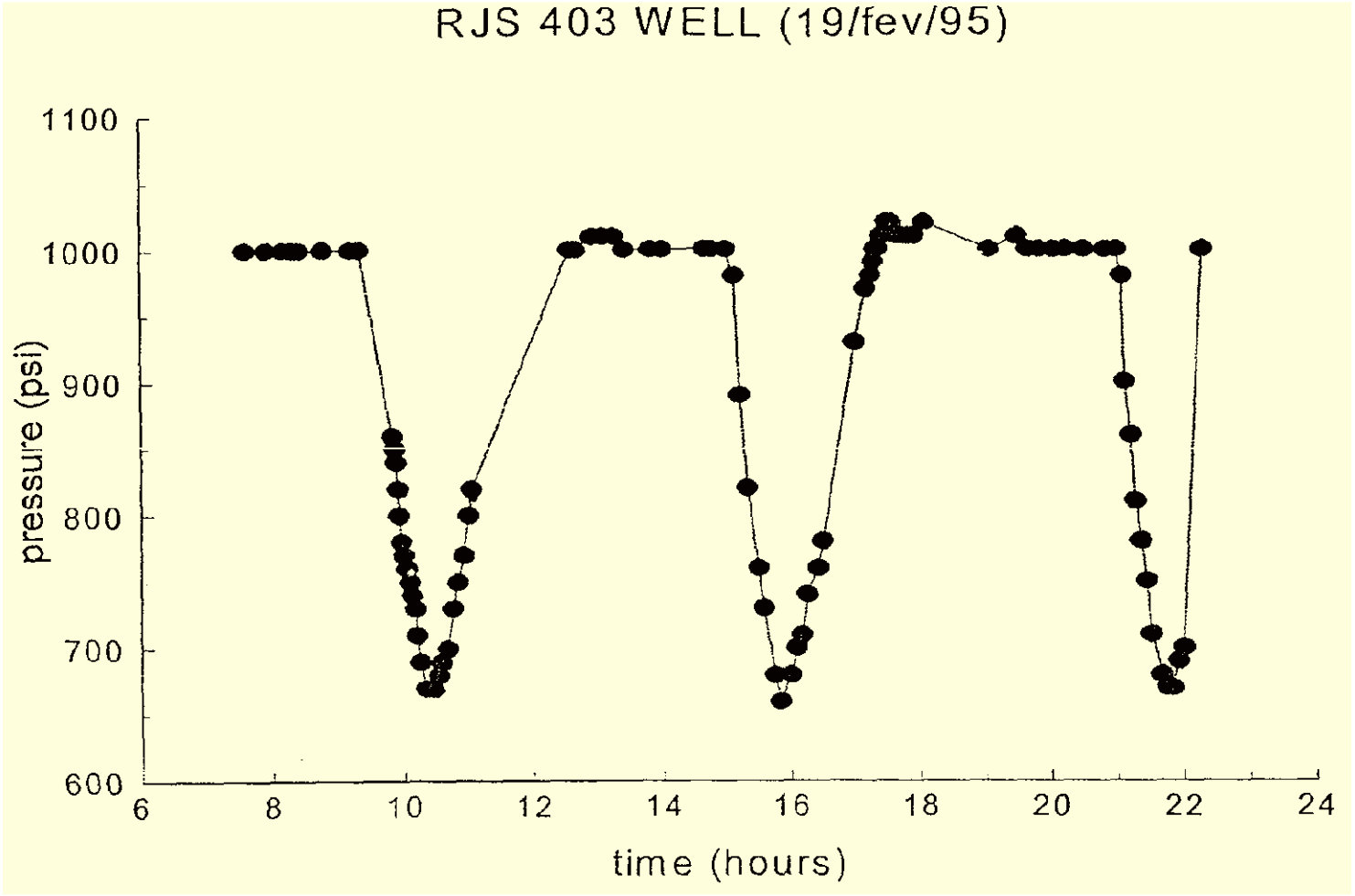

Production: 2400 *STB/d*. Mean pressure at “steady” state: 700 *psi*. Mean pressure with SS: 900 *psi*. Production loss: 800 *STB/d*.

Severe slugging classification

- SS1: the liquid slug length is greater to or equal to one riser length and maximum pipeline pressure is equal to the hydrostatic head of the riser (neglecting friction pressure drop).
- SS2 : the liquid length is less than one riser length, with intermittent gas penetration at the bottom of the riser.
- SS3: there is continuous gas penetration at the bottom of the riser; visually, the flow in the riser resembles normal slug flow, but pressure, slug lengths and frequencies reveal cyclic variations of smaller periods and amplitudes compared to SS1.
- OSC: there are cyclic pressure fluctuations without the spontaneous vigorous blowdown.

Severe slugging mitigation devices

- SS mainly controlled by dydrostatic pressure drop at the riser and compressibility at the pipeline. Mitigation devices:
  - Pressure increase at the separator: compresses the gas phase and makes the system less compressible. Disadvantage: reduction in production, as pressure difference between the reservoir and separator is the driving force.
  - Flow restriction in the riser (choke valve): in addition to the system pressure increase, any increase in flow rate at the top of the riser gives rise to an increase in frictional pressure drop across the valve, causing an additional stabilization effect. Reduction in production. System control action.
  - Gas injection: aeration of the liquid column and reduction of the pressure gradient. Relatively large gas flow rates are necessary. Pumping operational cost can be very signicant.
  - Self-lifting (Tangesdall *et al.*, 2002, 2003): gas transfer from the pipeline to the riser, without pumping power.
  - Venturi (Almeida & Gonçalves, 1999): flow acceleration at the pipeline, eliminating the stratified flow pattern.

Air-water model

- Model:
  - One-dimensional, isothermal flow and a mixture momentum equation in which gravitational and frictional terms are important.
  - Inertia and propagation of pressure waves were neglected both in the pipeline and riser (no-pressure-wave, NPW, approximation); pressure changes are felt instantaneously at any point.
  - Constant void fraction and pressure drop at the pipeline (taken from stationary state, stratified flow pattern).
- Improvements:
  - Inertial terms taken into account by using the rigid water-hammer approximation (not shown here).
  - Variable void fraction and pressure drop at the pipeline (not shown here).
  - Gas injection at the bottom of the riser.
  - Choke valve at the top of the riser.

Pipeline

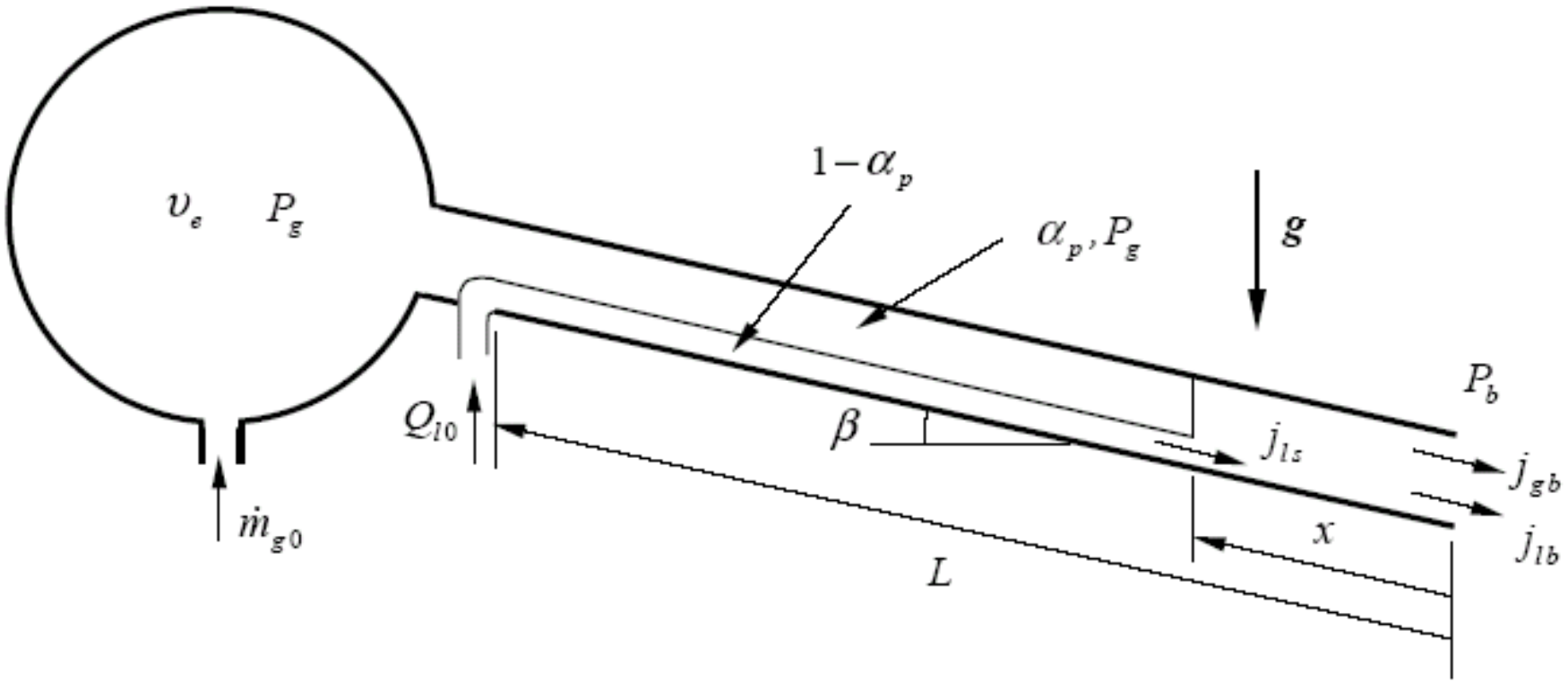

Pipeline equations

- Condition $x > 0$:

$$j_{g\,b} = 0 \qquad \frac{dx}{dt} = \frac{j_{l0} - j_{l\,b}}{\alpha_p}$$

$$\frac{dP_g}{dt} = \frac{-P_g \left(j_{l\,b} - j_{l0} \right) + \frac{T_g}{T_0} P_0\, j_{g0}}{(L - x)\,\alpha_p + L_e}$$

$$j_{l0} = \frac{Q_{l0}}{A} \qquad j_{g0} = \frac{R_g\, T_0\, \dot{m}_{g0}}{P_0\, A} \qquad L_e = \frac{v_e}{A}$$

$$P_b = P_g + \rho_l\, g\, x\ \text{sen}\,\beta$$

Pipeline equations

- Condition $x = 0$:

$$j_{lb} = j_{l0}$$

$$\frac{dP_g}{dt} = \frac{-P_g\, j_{g\,b} + \frac{T_g}{T_0} P_0\, j_{g0}}{L\,\alpha_p + L_e}$$

$$P_b = P_g$$

Pipeline commutation

- Commutation from $x = 0$ to $x > 0$:

$$j^-_{g\,b} = j^+_{g\,b} = 0 \qquad j^+_{l\,b} = j^-_{l\,b} \qquad \frac{dx^+}{dt} = 0$$

- Commutation from $x > 0$ to $x = 0$:

$$j^+_{g\,b} = -\alpha_p \frac{dx^-}{dt} \qquad j^+_{l\,b} = j^-_{l\,b} + \alpha_p \frac{dx^-}{dt}$$

$$\frac{dx^+}{dt} = 0 \qquad j^-_{g\,b} = 0$$

- Commutations guarantee continuity in pressure and time derivative of pressure at the bottom of the riser.

Pipeline local equilibrium condition

- Momentum balance in stratified flow (Taitel, 1976) for stationary state:

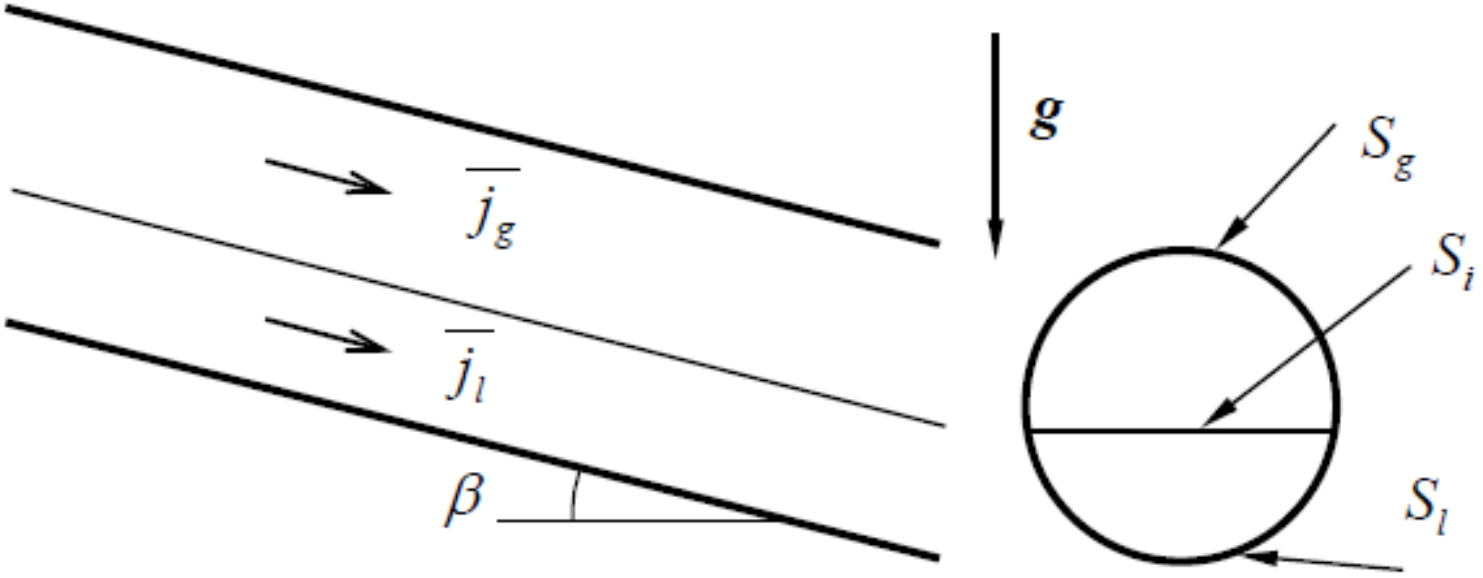

$$\tau_{w\,g}\,\frac{S_g}{\alpha_p} - \tau_{w\,l}\,\frac{S_l}{1-\alpha_p} + \tau_i\,S_i\left(\frac{1}{1-\alpha_p}+\frac{1}{\alpha_p}\right) + (\rho_l-\rho_g)\;A\,g\;\text{sen}\,\beta = 0$$

Riser

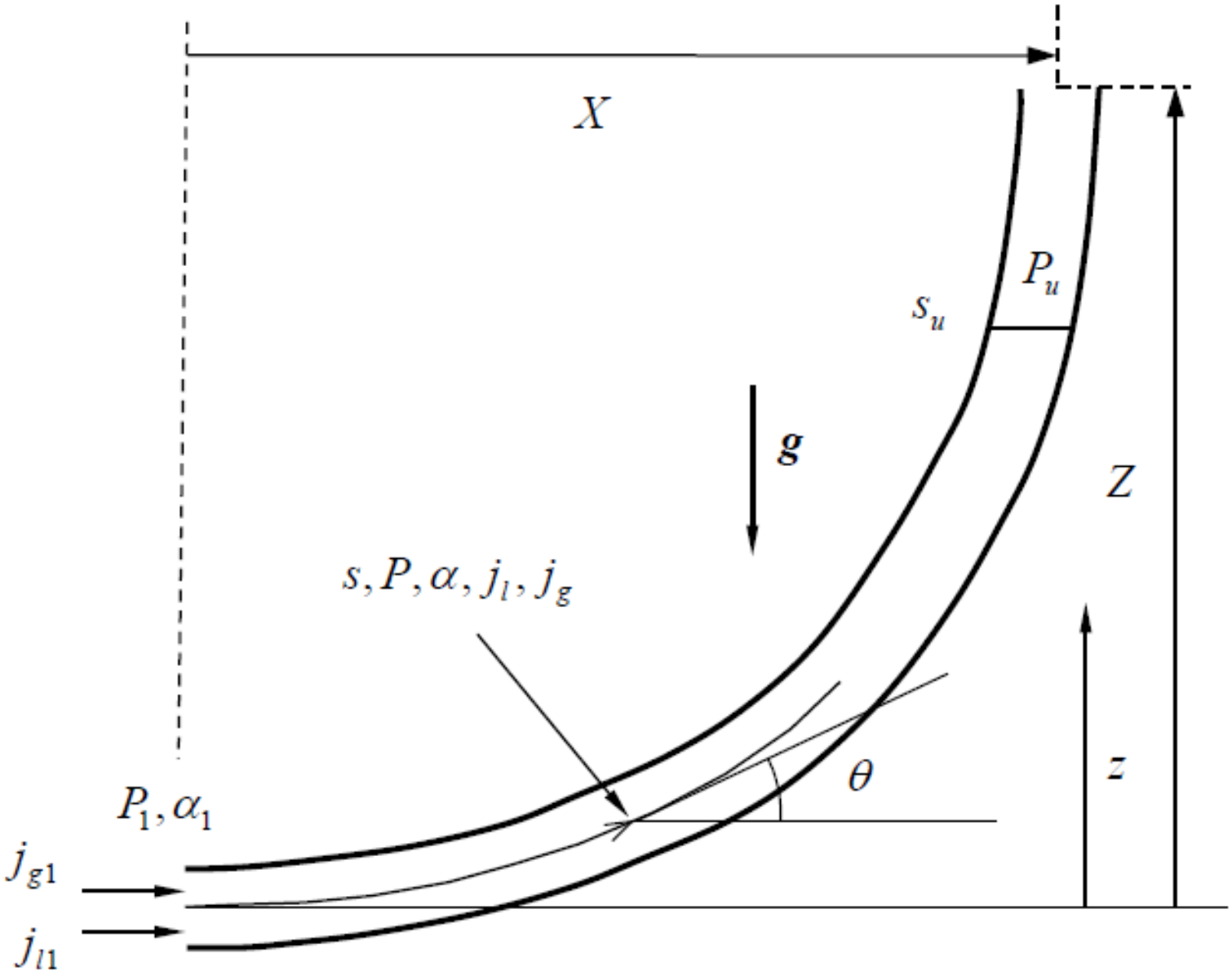

Riser equations

- Continuity:

$$-\frac{\partial \alpha}{\partial t} + \frac{\partial j_l}{\partial s} = 0 \qquad \frac{\partial}{\partial t}(P\,\alpha) + \frac{\partial}{\partial s}(P\,j_g) = 0$$

- Mixture linear momentum:

$$\frac{\partial P}{\partial s} = -\rho_m \left(g\ \mathrm{sen}\,\theta + 2\,\frac{f_m}{D}\,j\ |j| \right)$$

$$\rho_m = \rho_l\,(1-\alpha) + \rho_g\,\alpha \qquad \rho_g = \frac{P}{R_g\,T_g}$$

- Closure law (drift flux model):

$$j_g = u_g\,\alpha = \alpha\,(C_d\,j + U_d)$$

$$j_l = j - j_g = u_l\,(1-\alpha) = (1-\alpha\,C_d)\,j - \alpha\,U_d$$

Characteristic values

- For a general drift flux correlation:

$$C_d = C_d\left(\alpha,\, j_g,\, j_l,\, P,\, \theta\right)$$

$$U_d = U_d\left(\alpha,\, j_g,\, j_l,\, P,\, \theta\right)$$

- Characteristic direction for the NPW approximation is:

$$e_1 = \frac{\partial j_g}{\partial \alpha}$$

- If the drift coefficients are independent of void fraction:

$$\frac{\partial j_g}{\partial \alpha} = \frac{j_g}{\alpha} = u_g$$

Drift flux correlation

- Bendiksen correlation (1984): $Fr_j = \dfrac{j}{\sqrt{g\,D}}$

$$C_d = \begin{cases} 1.05 + 0.15\,\sin\theta & \text{for } Fr_j < 3.5 \\ 1.2 & \text{for } Fr_j > 3.5 \end{cases}$$

$$U_d = \begin{cases} \sqrt{g\,D}\,(0.35\,\sin\theta + 0.54\,\cos\theta) & \text{for } Fr_j < 3.5 \\ 0.35\,\sqrt{g\,D}\,\sin\theta & \text{for } Fr_j > 3.5 \end{cases}$$

- Characteristic equations become:

$$\frac{D_g\alpha}{Dt} + \alpha\,\frac{\partial}{\partial s}\,(C_d\,j + U_d) - \frac{\partial j}{\partial s} = 0$$

$$\alpha\,\frac{D_g P}{Dt} + P\,\frac{\partial j}{\partial s} = 0$$

$$\frac{D_g}{Dt} = \frac{\partial}{\partial t} + u_g\,\frac{\partial}{\partial s}$$

Riser, gas lift

- Gas injection aerates the liquid column, reduce the pressure gradient and can stabilize the flow in severe slugging, although relatively large gas flow rates are necessary. Gas injection at position s_l introduces discontinuities in position in the gas superficial velocity and void fraction:

$$j_g^+ = j_g^- + \frac{T_g}{T_0}\frac{P_0}{P_l}\, j_{g0\,l} \qquad \alpha^+ = \frac{j_g^+}{(C_d\, j + U_d)^+}$$

$$j_{g0\,l} = \frac{R_g\, T_0\, \dot{m}_{gl}}{P_0\, A}$$

Riser, choke valve

- In normal operation in petroleum production systems the choke valve controls the flow. Choking can stabilize the flow by increasing the back pressure. For low pressures, typical of air-water laboratory systems, the valve operates in subcritical condition.

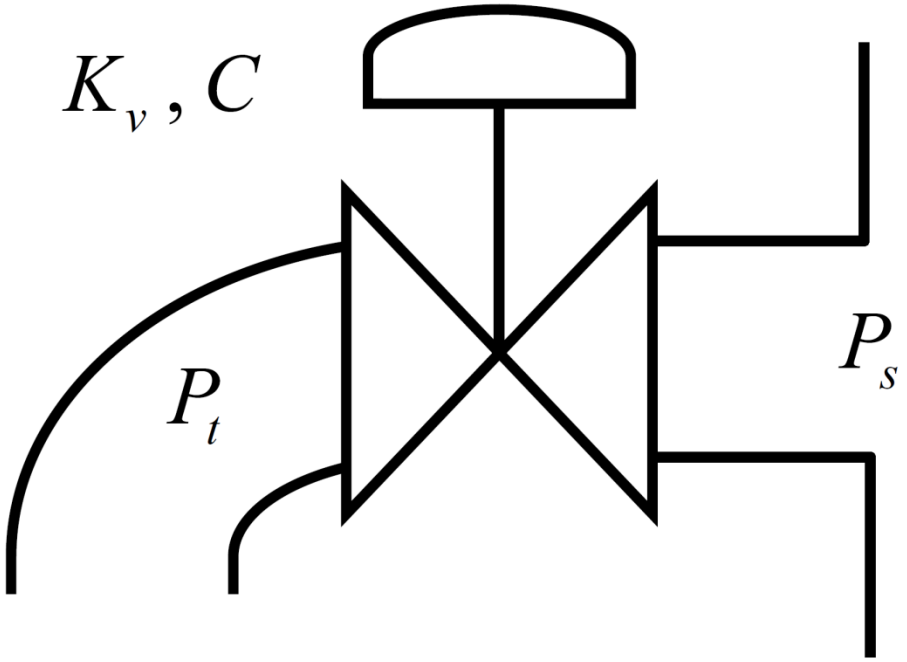

$$P_t - P_s = K_v \frac{1}{2} \rho_{mt} j_t |j_t|$$

(homogeneous)

$$P_t - P_s = C j_{lt} |j_{lt}|$$

(Jansen *et al*., 1996)

Pipeline-riser coupling

$$P(s=0,\,t) = P_b(t)$$

$$j_g(s=0,\,t) = j_{g\,b}(t) \qquad j_l(s=0,\,t) = j_{l\,b}(t)$$

$$\alpha(s=0,\,t) = \alpha_b(t) = \frac{j_{g\,b}}{C_{d\,b}\,j_b + U_{d\,b}}$$

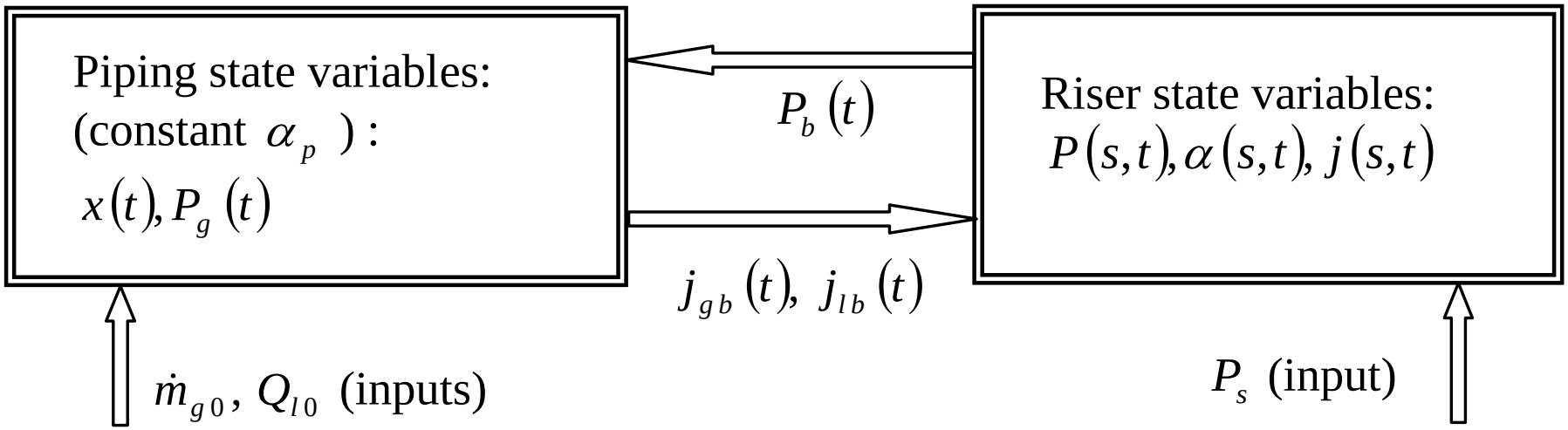

Stationary state

- The stationary state, when stable, is the steady state flow operational regime. It is used as the initial condition for the transient simulations and also as the base solution for the linear stability analysis.
- For the pipeline:

$$\tilde{j}_{lb} = j_{l0} \qquad \tilde{j}_{gb} = \frac{T_g}{T_0}\frac{P_0}{\tilde{P}_b} j_{g0}$$

- For the riser:

$$\tilde{j}_l = j_{l0}$$

$$\tilde{j}_g = \begin{cases} \dfrac{T_g}{T_0}\dfrac{P_0}{\tilde{P}} j_{g0} & \text{for } s < s_l \\ \dfrac{T_g}{T_0}\dfrac{P_0}{\tilde{P}} \left(j_{g0} + j_{g0\,l}\right) & \text{for } s > s_l \end{cases}$$

Stationary state

- For the riser (continued):

$$\tilde{\alpha} = \begin{cases} \dfrac{j_{g0}}{\tilde{C}_d\, j_{g0} + \left(j_{l0} + \tilde{U}_d\right) \dfrac{T_0}{T_g} \dfrac{\tilde{P}}{P_0}} & \text{for } s < s_l \\ \dfrac{j_{g0} + j_{g0\,l}}{\tilde{C}_d\, \left(j_{g0} + j_{g0\,l}\right) + \left(j_{l0} + \tilde{U}_d\right) \dfrac{T_0}{T_g} \dfrac{\tilde{P}}{P_0}} & \text{for } s > s_l \end{cases}$$

$$\frac{\partial \tilde{P}}{\partial s} = -\tilde{\rho}_m \left(g\, \sin\theta + 2\, \frac{\tilde{f}_m}{D}\, \tilde{j}^2 \right)$$

Experiments

Wordsworth et al. (1998) for catenary risers:

$$Z = 9.886\,m$$

$$X = 6.435\,m$$

$$s_t = 12.5463\,m$$

$$D = 5.25018 \times 10^{-2}\,m$$

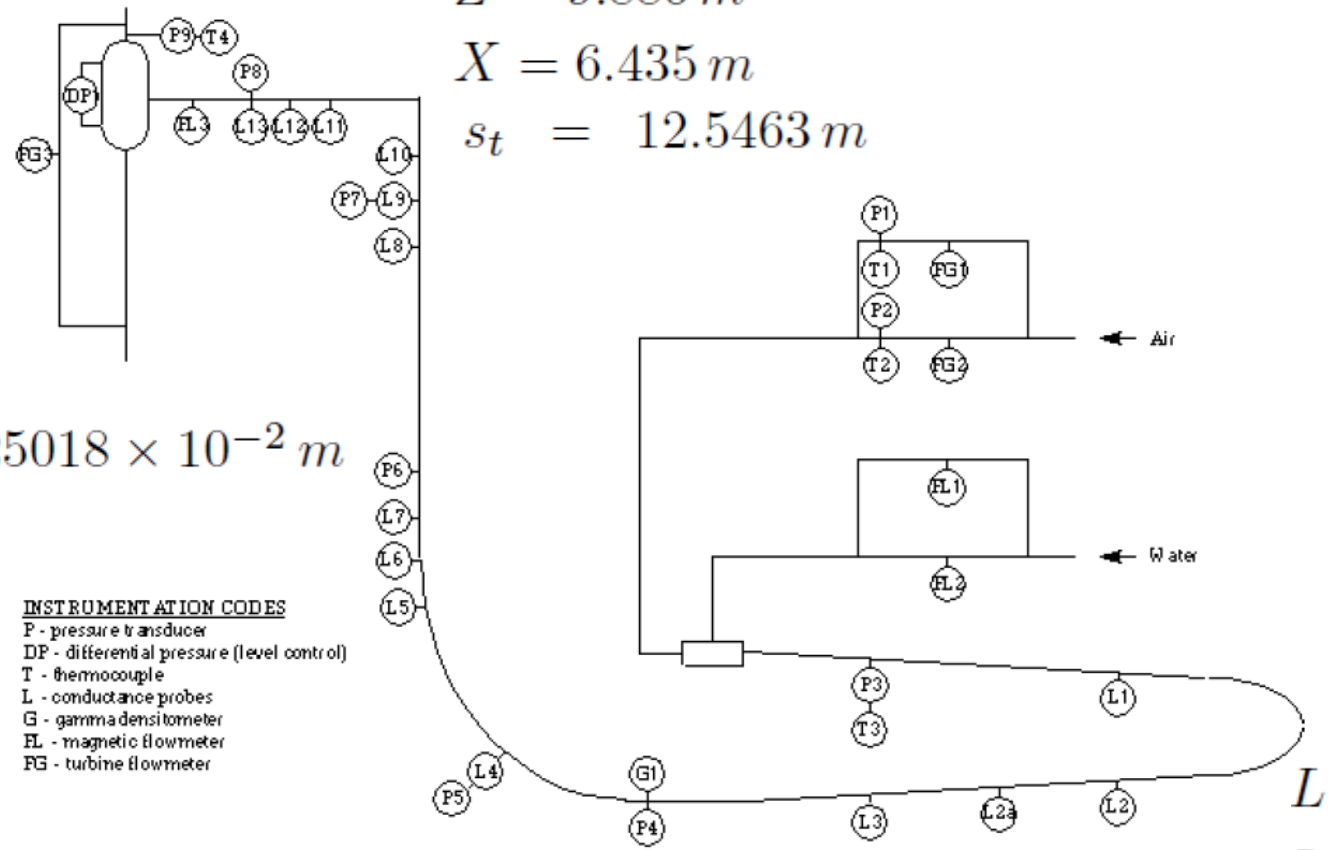

$$L = 57.4\,m$$

$$L_e = 0\,m$$

$$\beta = 2^o$$

Figure 1.10: Schematic of the test facility (Wordsworth *et al.*, 1998).

Experiments

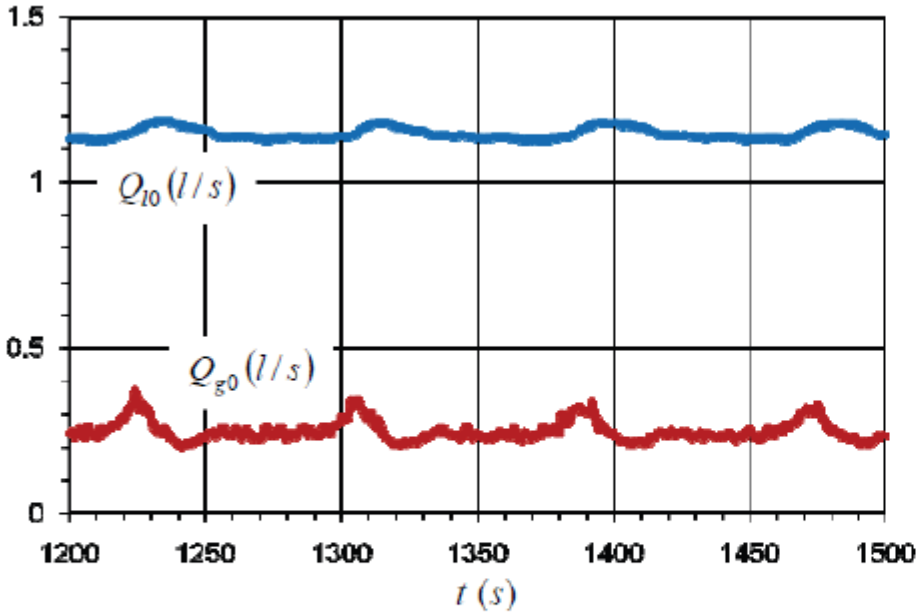

(*a*) Inlet flows.

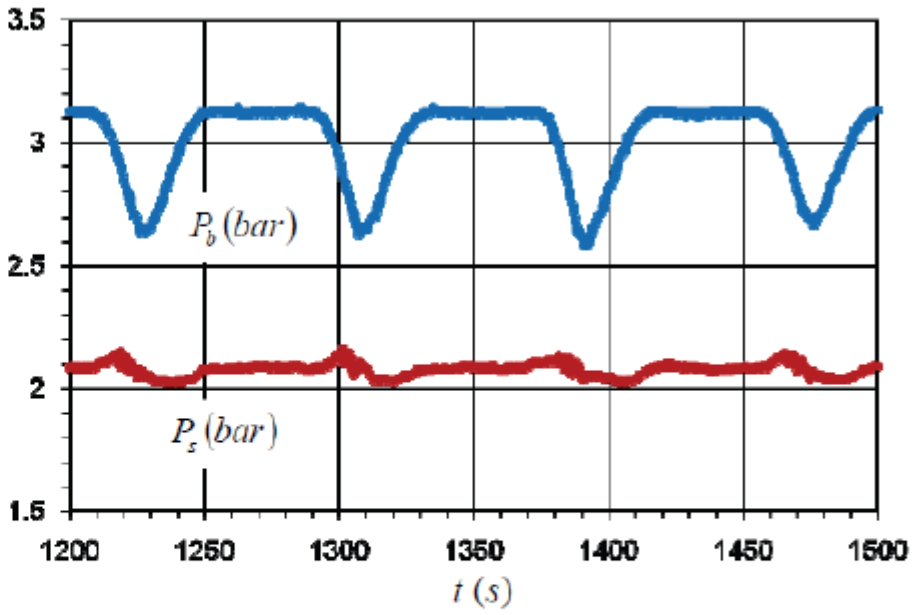

(*b*) Pressures.

Figure 1.11: Experimental history for SS1 (case 2, Table 1.3).

Experiments

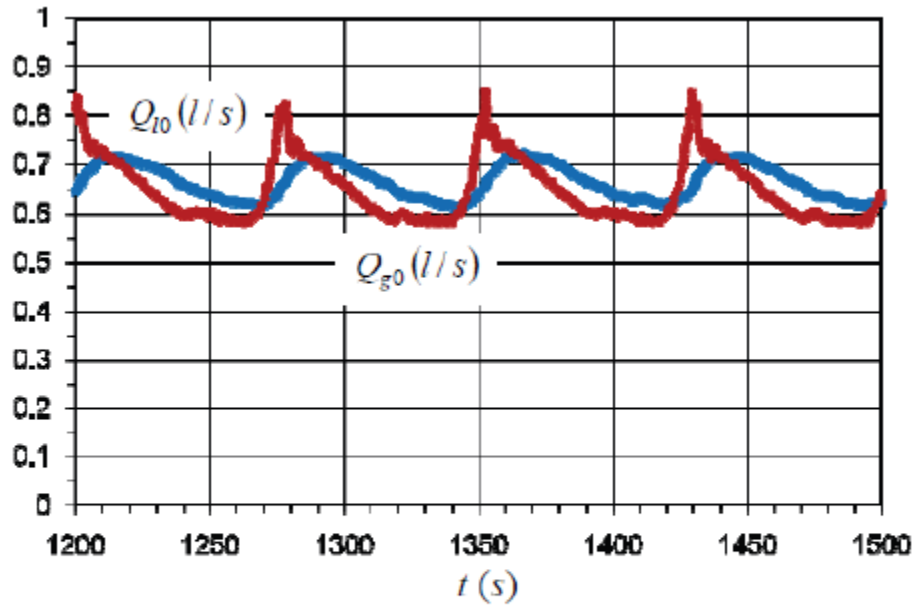

(*a*) Inlet flows.

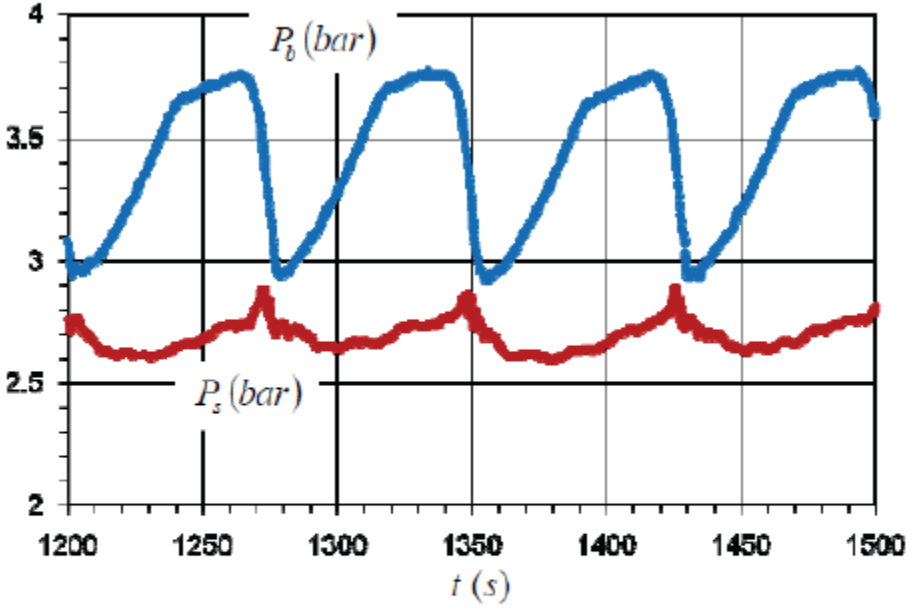

(*b*) Pressures.

Figure 1.12: Experimental history for SS2 (case 7, Table 1.4).

Experiments

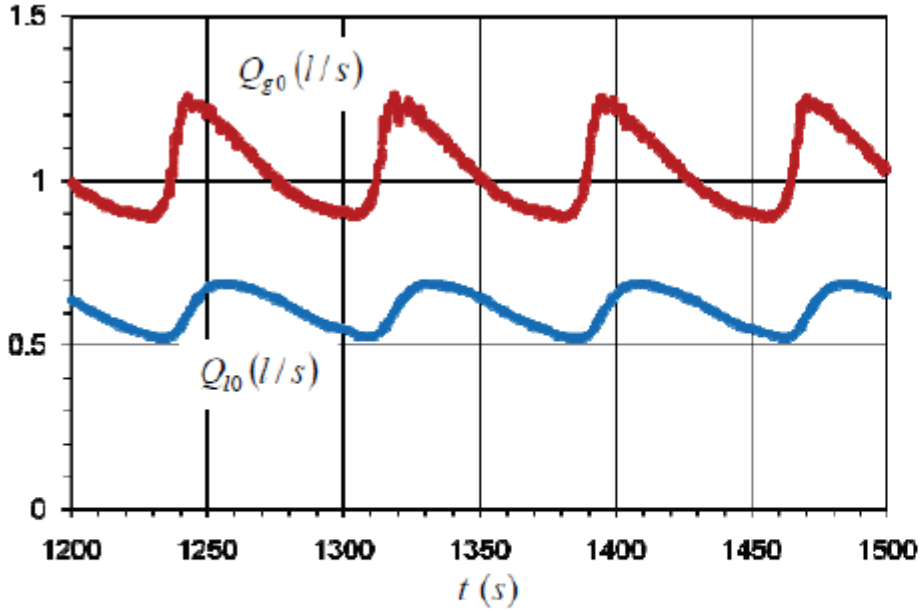

(*a*) Inlet flows.

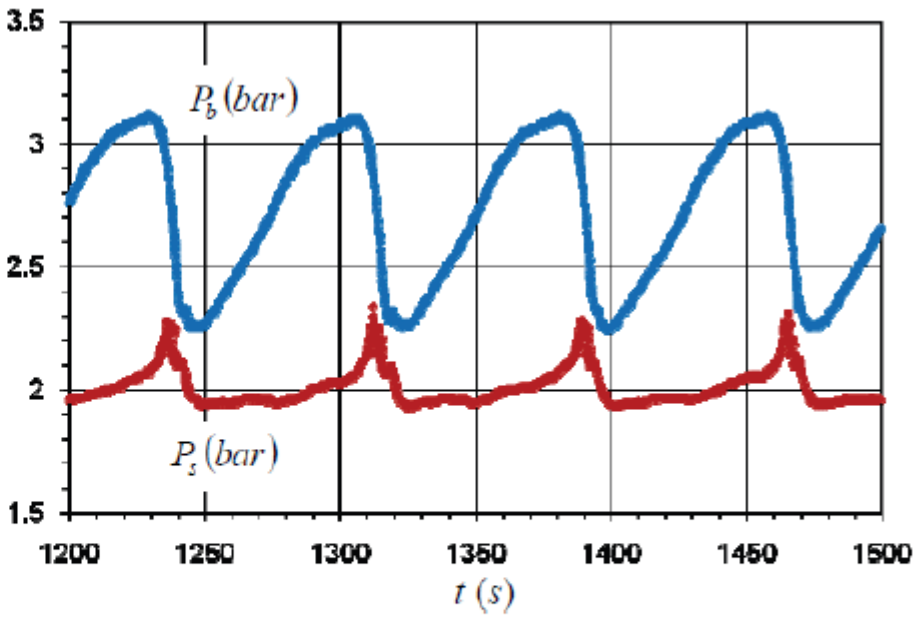

(*b*) Pressures.

Figure 1.13: Experimental history for SS3 (case 11, Table 1.3).

Experiments

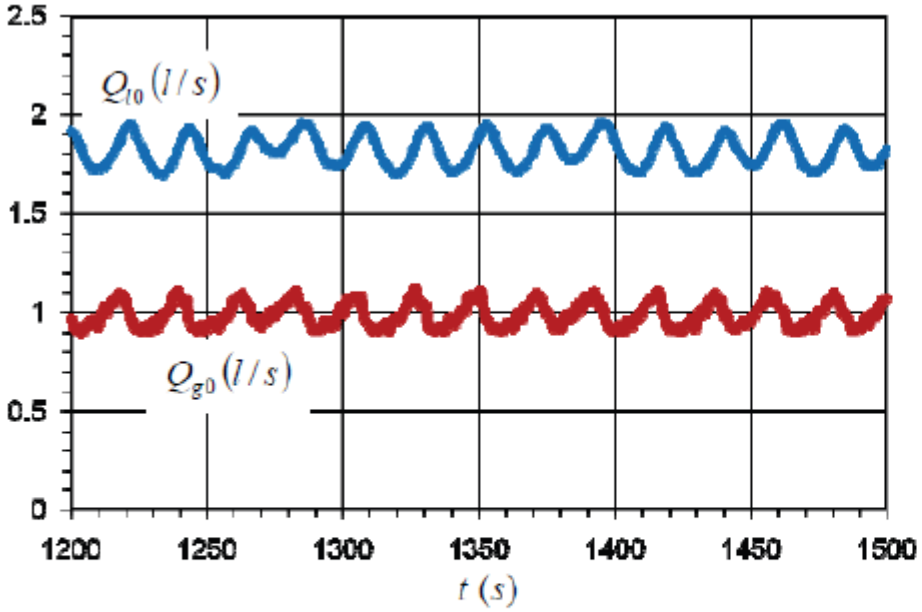

(*a*) Inlet flows.

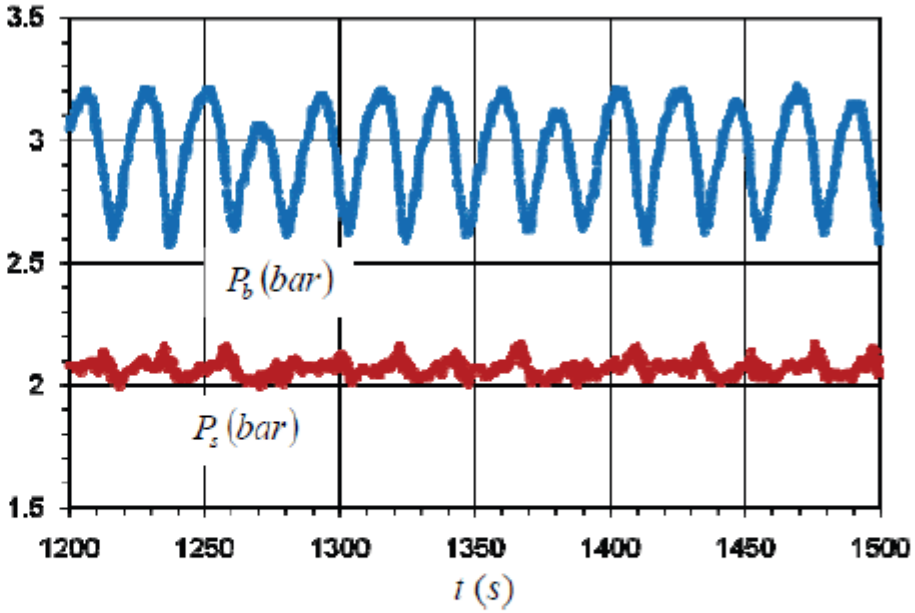

(*b*) Pressures.

Figure 1.14: Experimental history for OSC (case 17, Table 1.3).

Experiments

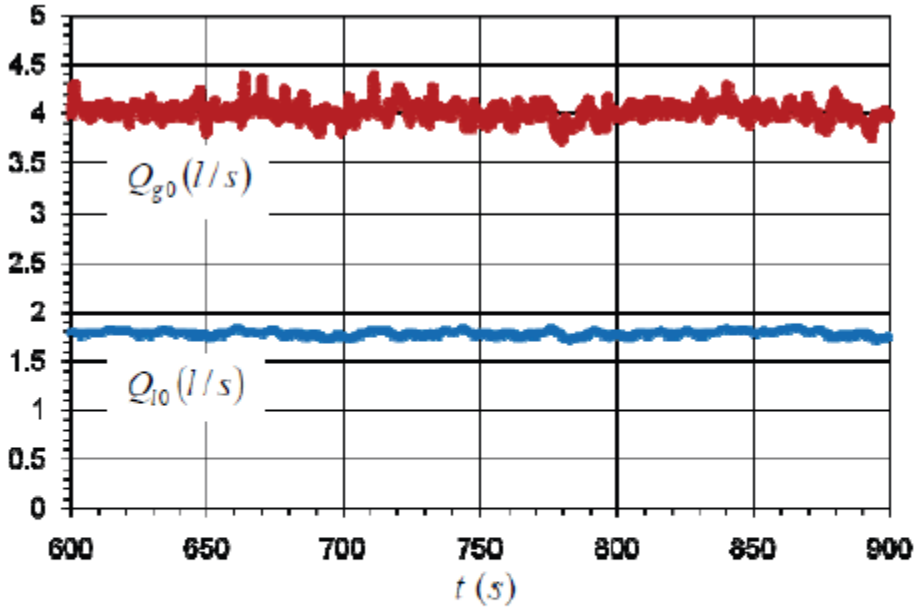

(*a*) Inlet flows.

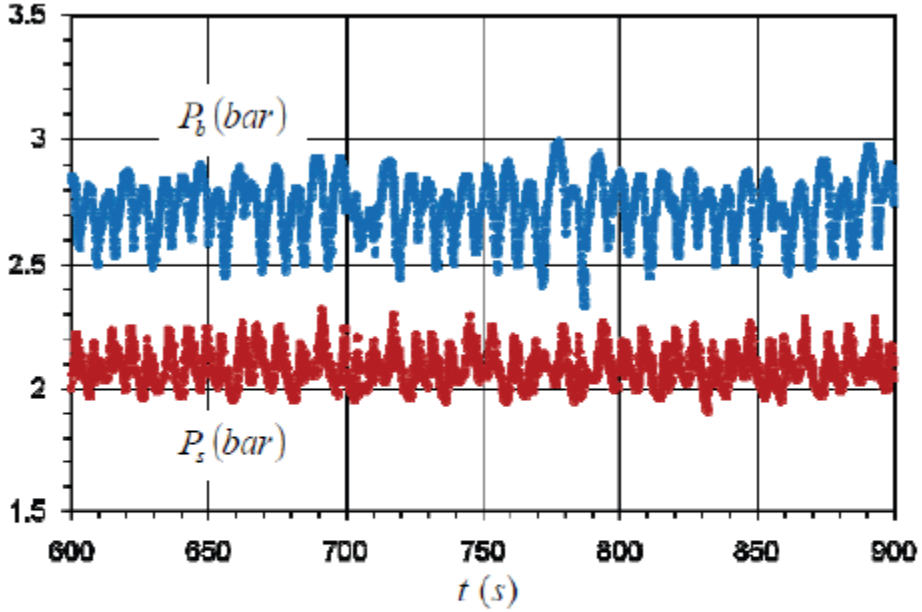

(*b*) Pressures.

Figure 1.15: Experimental history for slug flow (case 14, Table 1.3).

Experiments

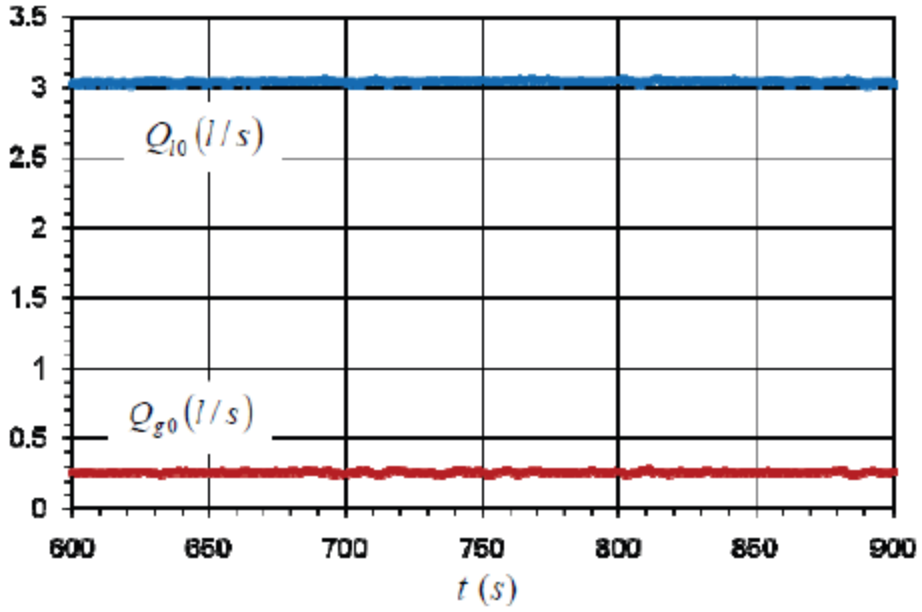

(*a*) Inlet flows.

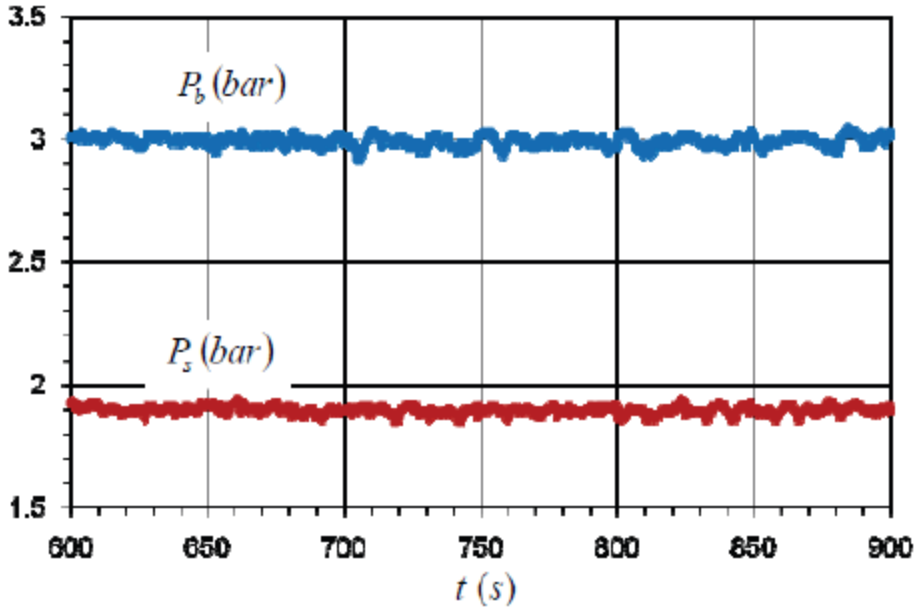

(*b*) Pressures.

Figure 1.16: Experimental history for plug flow (case 16, Table 1.3).

Experiments

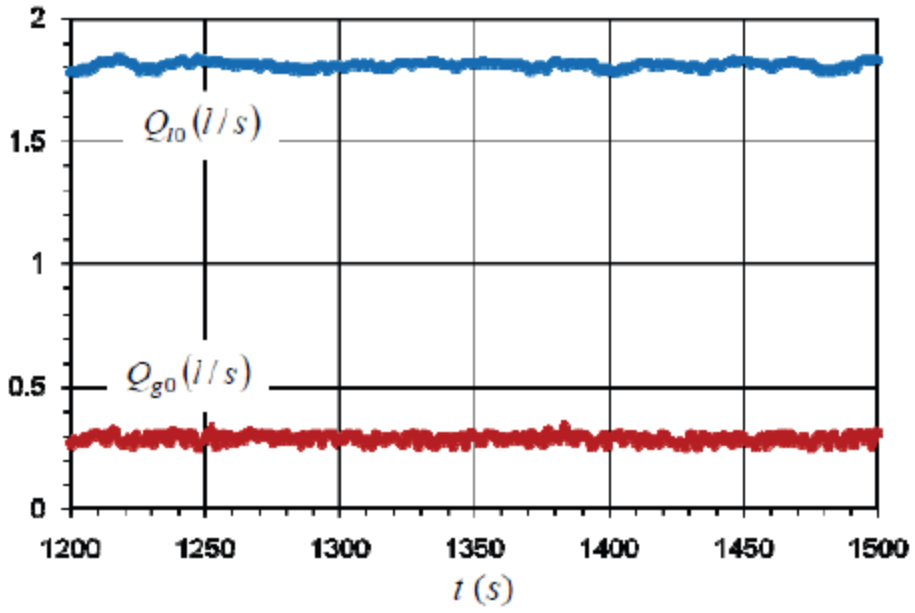

(*a*) Inlet flows.

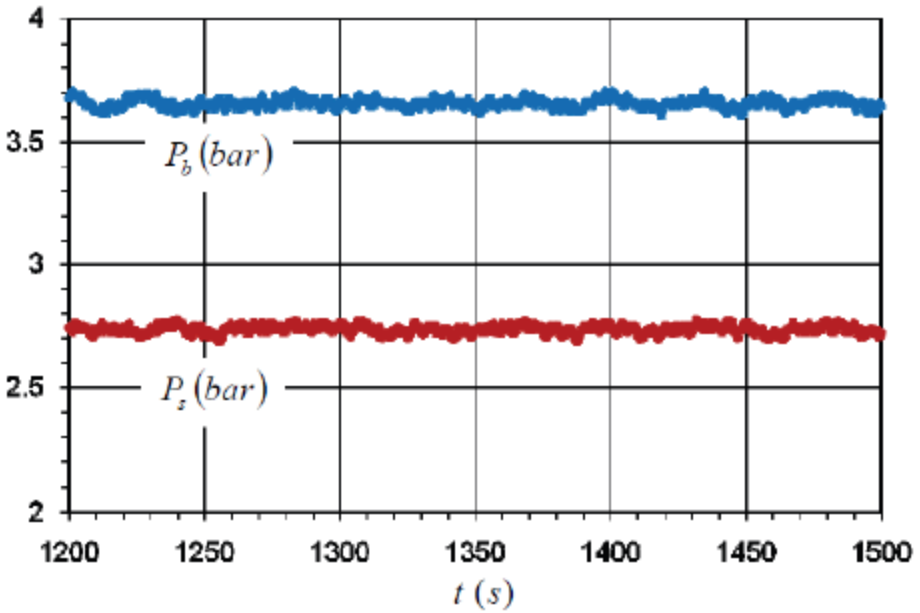

(*b*) Pressures.

Figure 1.17: Experimental history for bubbly flow (case 20, Table 1.4).

Experiments

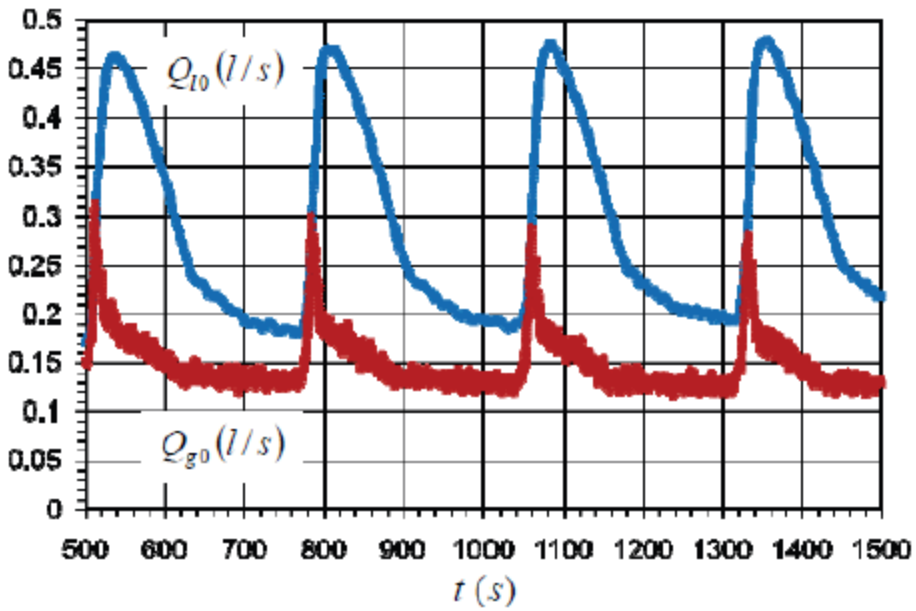

(*a*) Inlet flows.

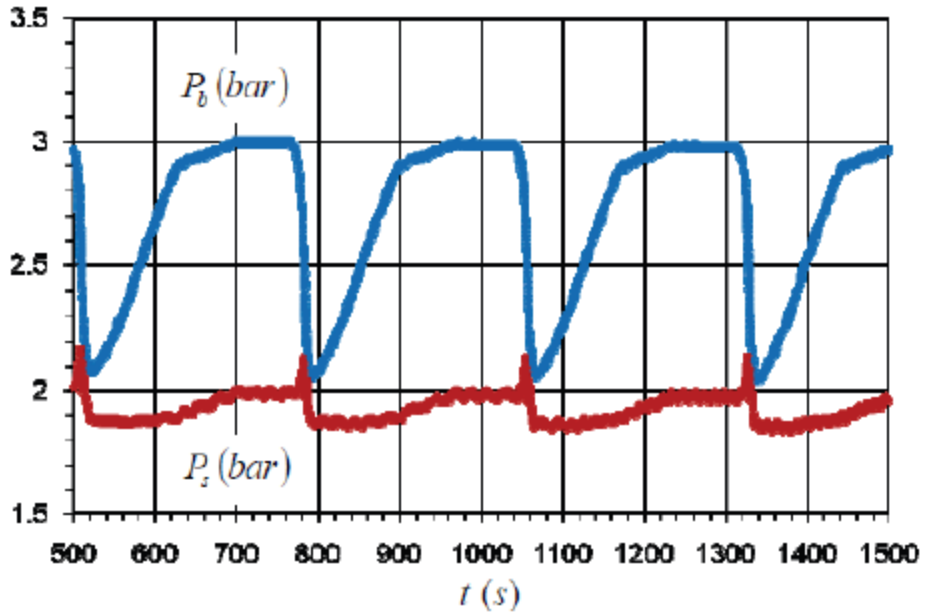

(*b*) Pressures.

Figure 1.22: Experimental history for case 4, Table 1.3.

Controlability of the boundary conditions!

Severe slugging pattern recognition

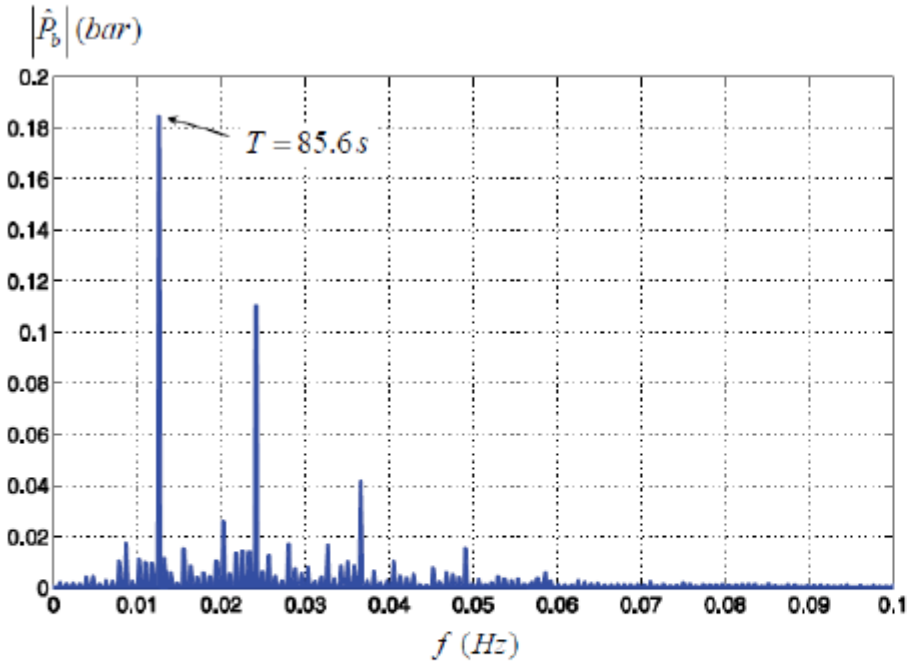

(*a*) SS1 (case 2, Table 1.3).

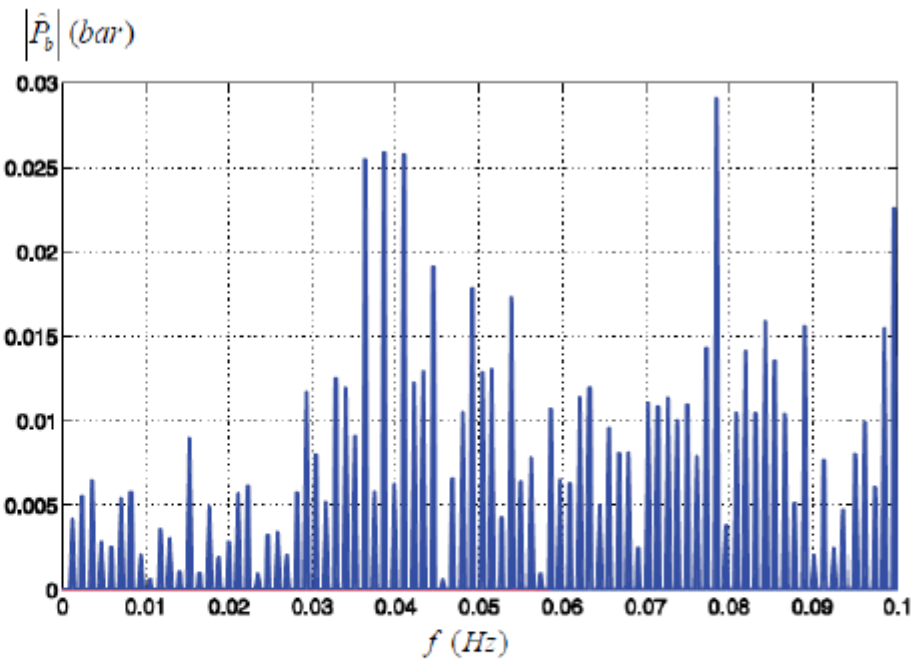

(*b*) Slug flow (case 14, Table 1.3).

Figure 1.18: FFT for different pressures histories.

Discretization

- Moving grid method between nodes 1 and *N*-1.
- Variable time step (method of characteristics), satisfying CFL (Courant–Friedrichs–Lewy) condition.
- Implicit scheme, predictor-corrector method for non-linearities.

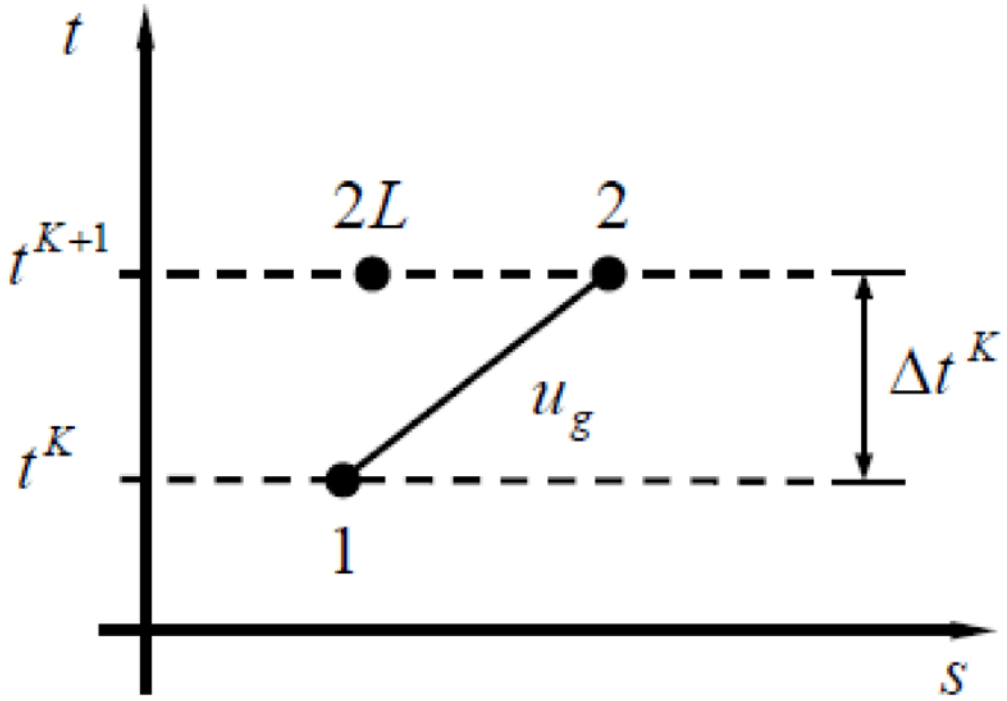

Simulations

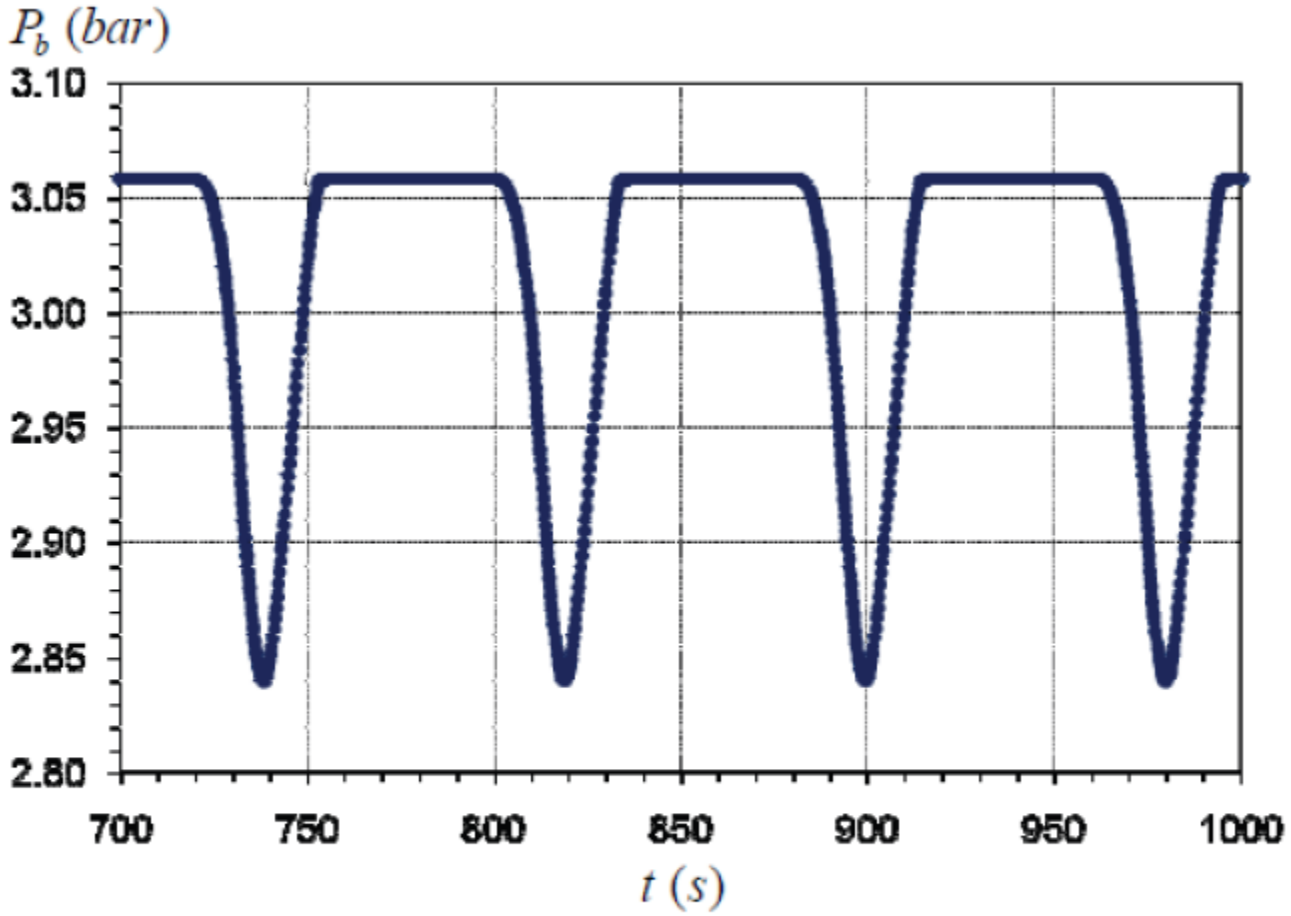

Figure 1.20: Simulated limit cycle, pressure at the bottom of the riser (type SS1, case 2, Table 1.3). $T_{sim} = 80{,}4\ s$ $T_{exp} = 85{,}6\ s$

Simulations

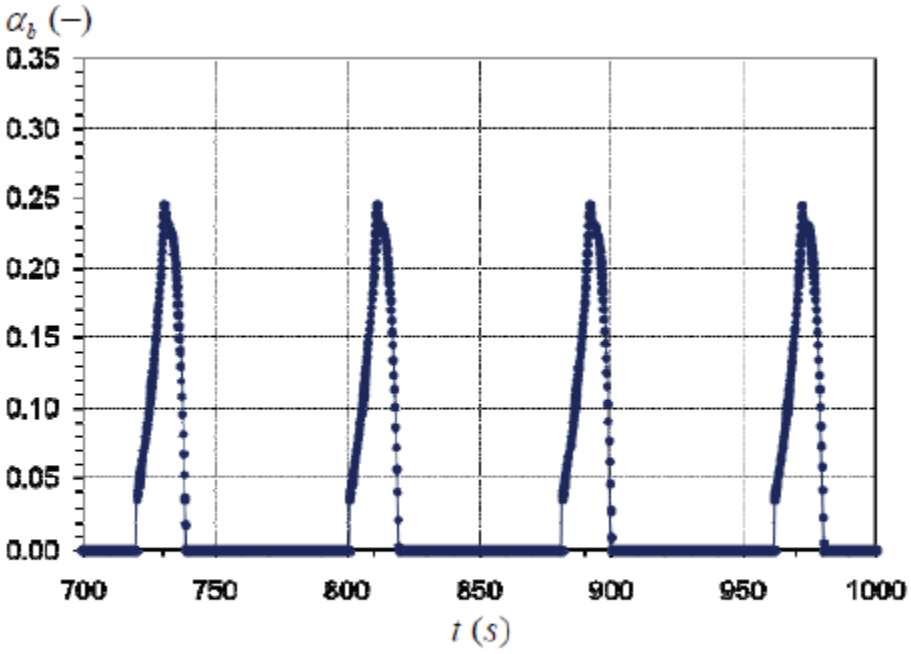

(a)

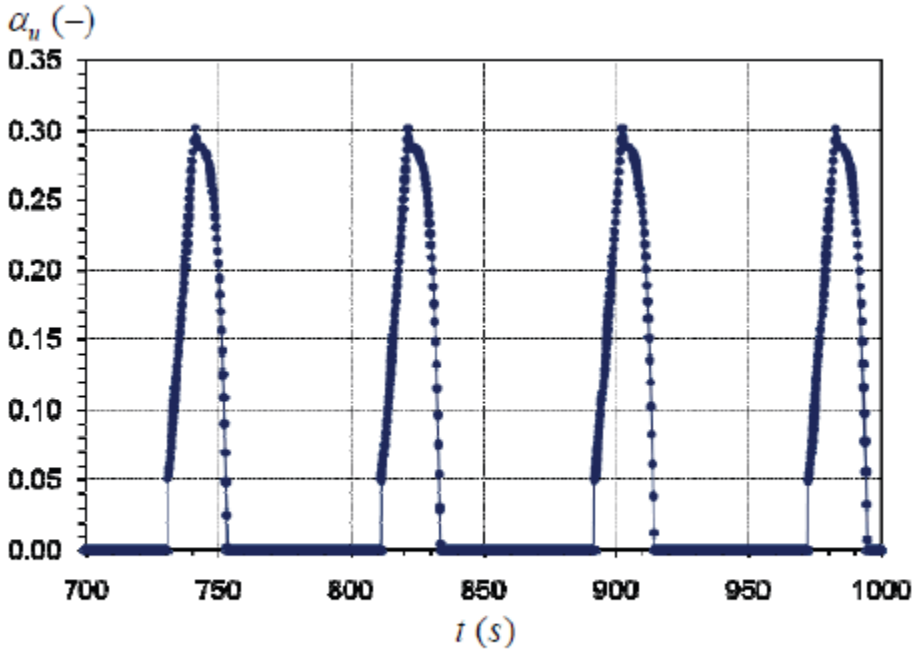

(b)

Simulations

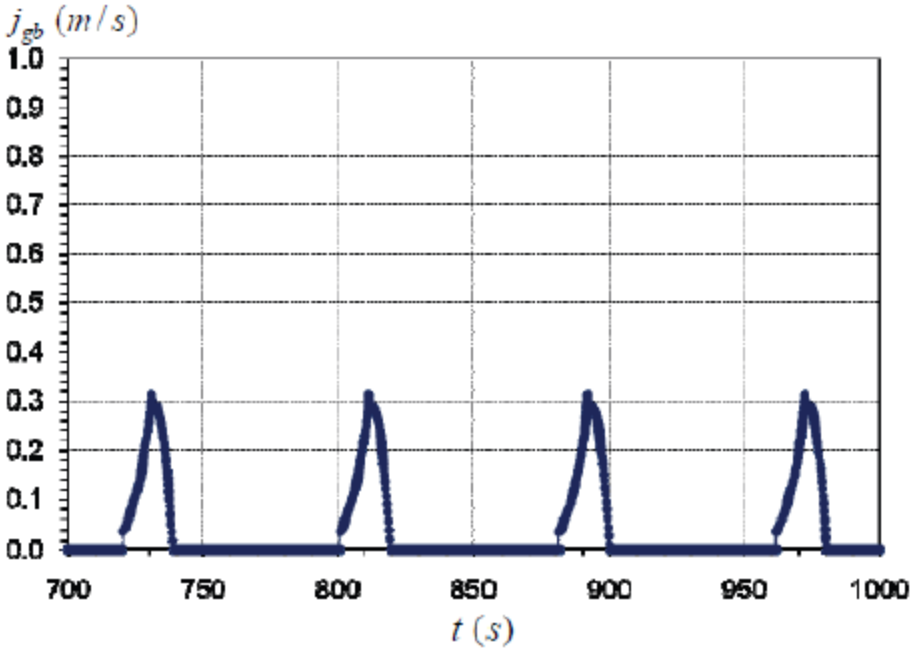

(c)

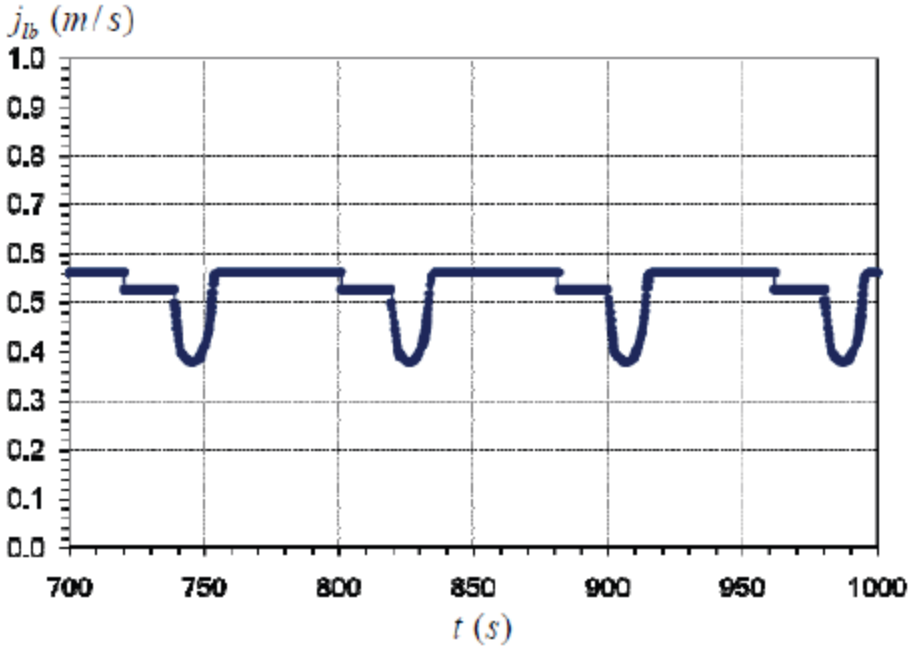

(d)

Simulations

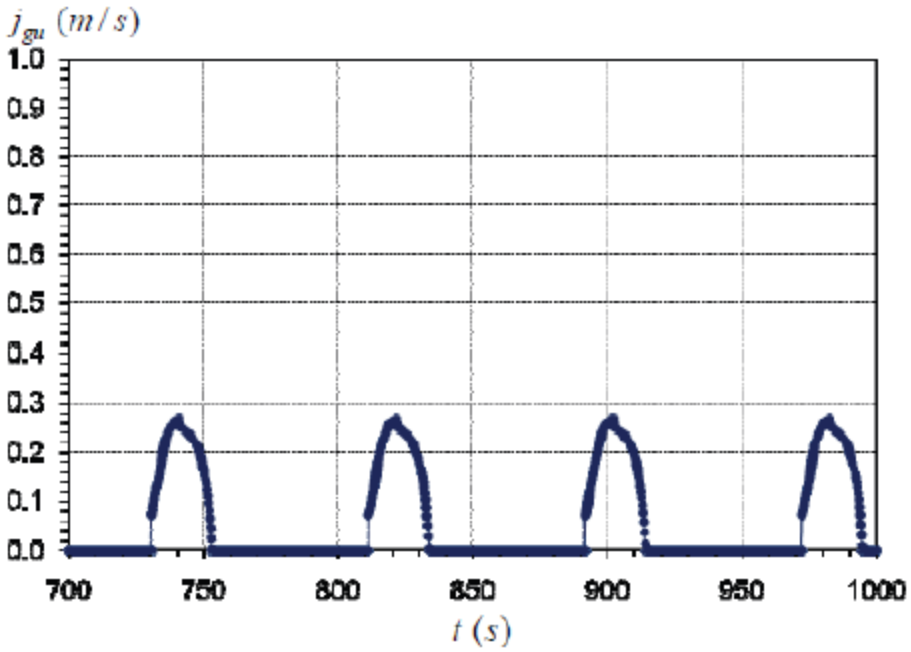

(e)

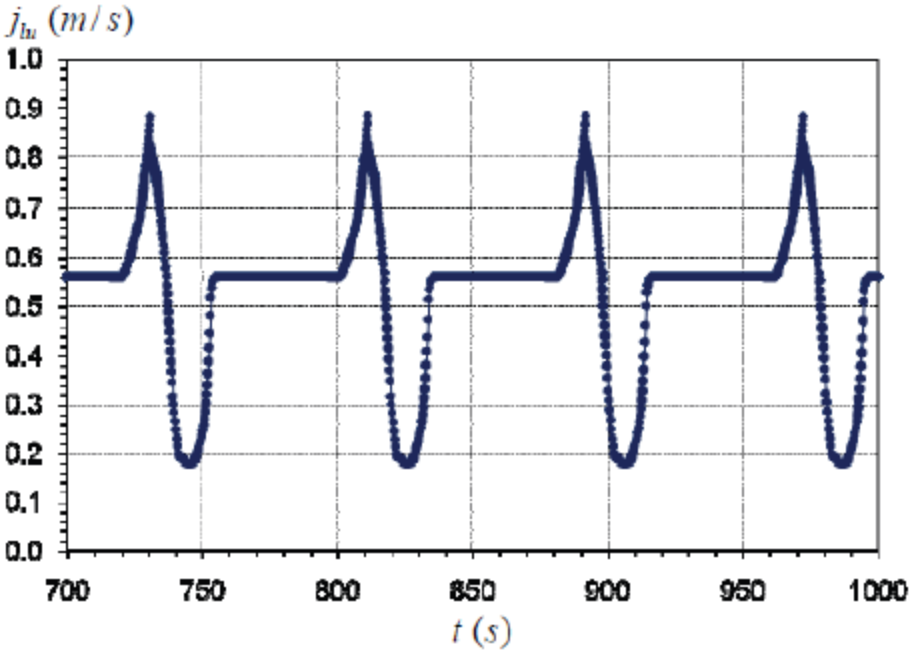

(f)

Simulations

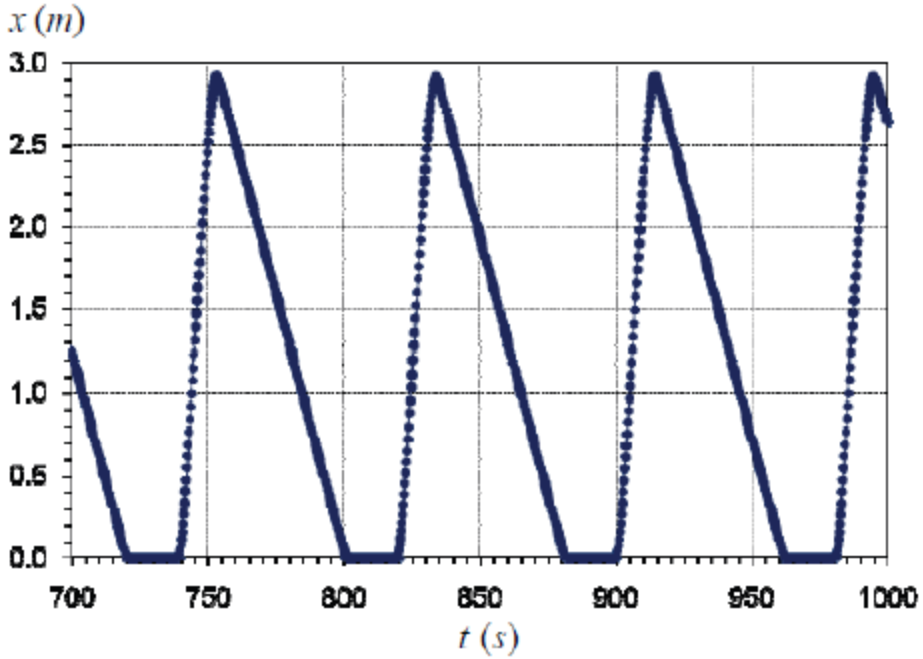

(g)

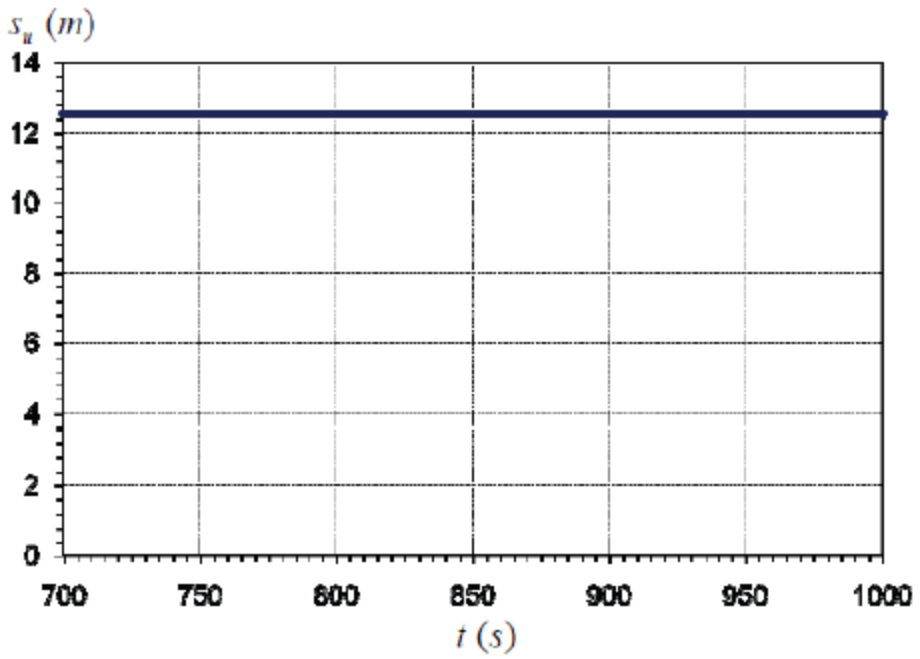

(h)

Stability maps

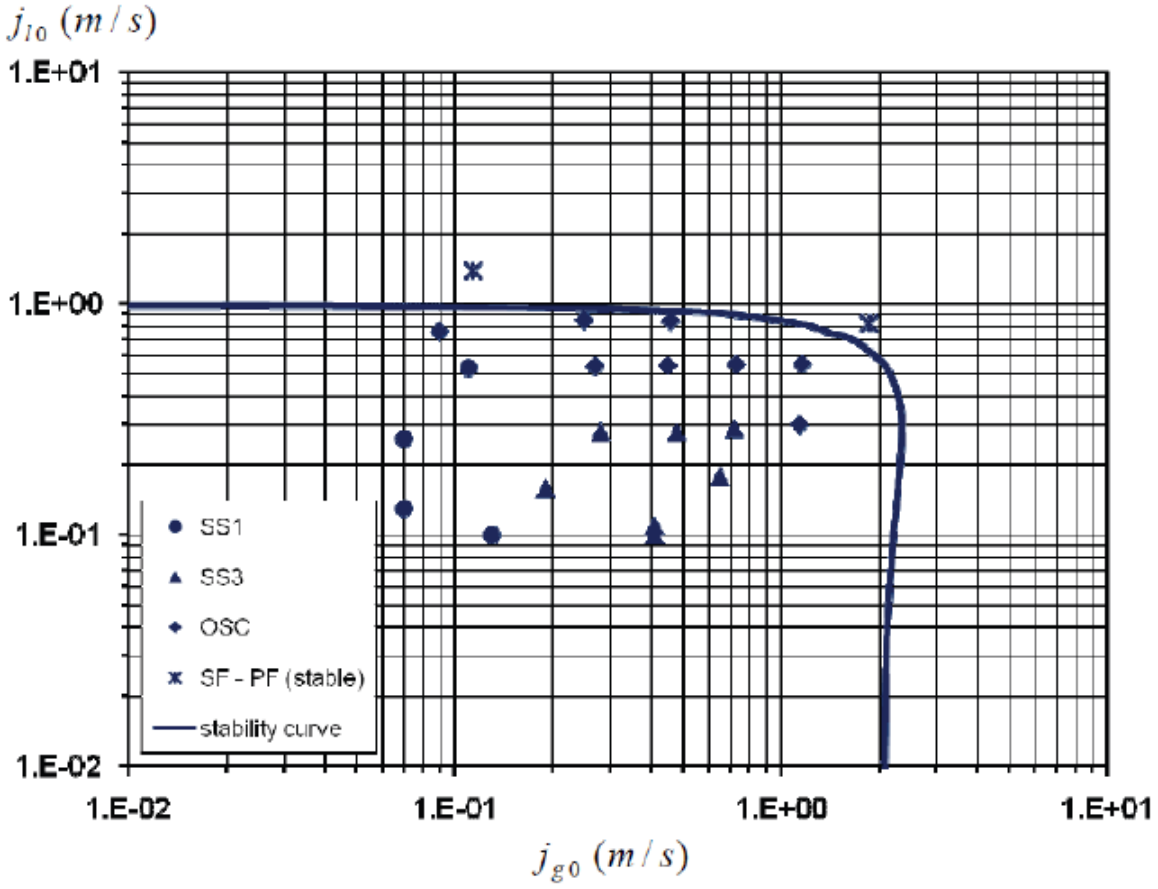

Figure 1.23: Experimental data (Table 1.3) and stability map for $P_s = 2.013\,bara$ and $T = 293\,K$.

Stability maps

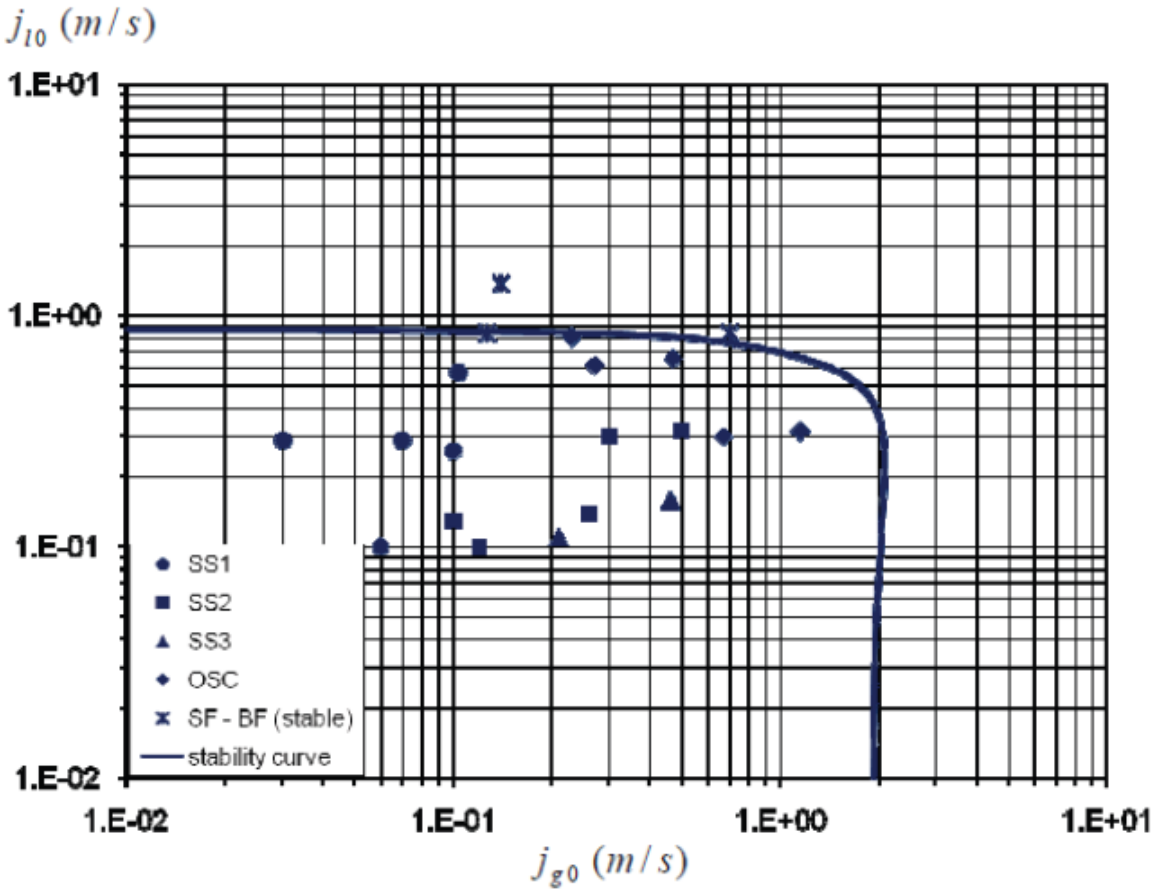

Figure 1.24: Experimental data (Table 1.4) and stability map for $P_s = 2.70\,bara$ and $T = 293\,K$.

Stability maps

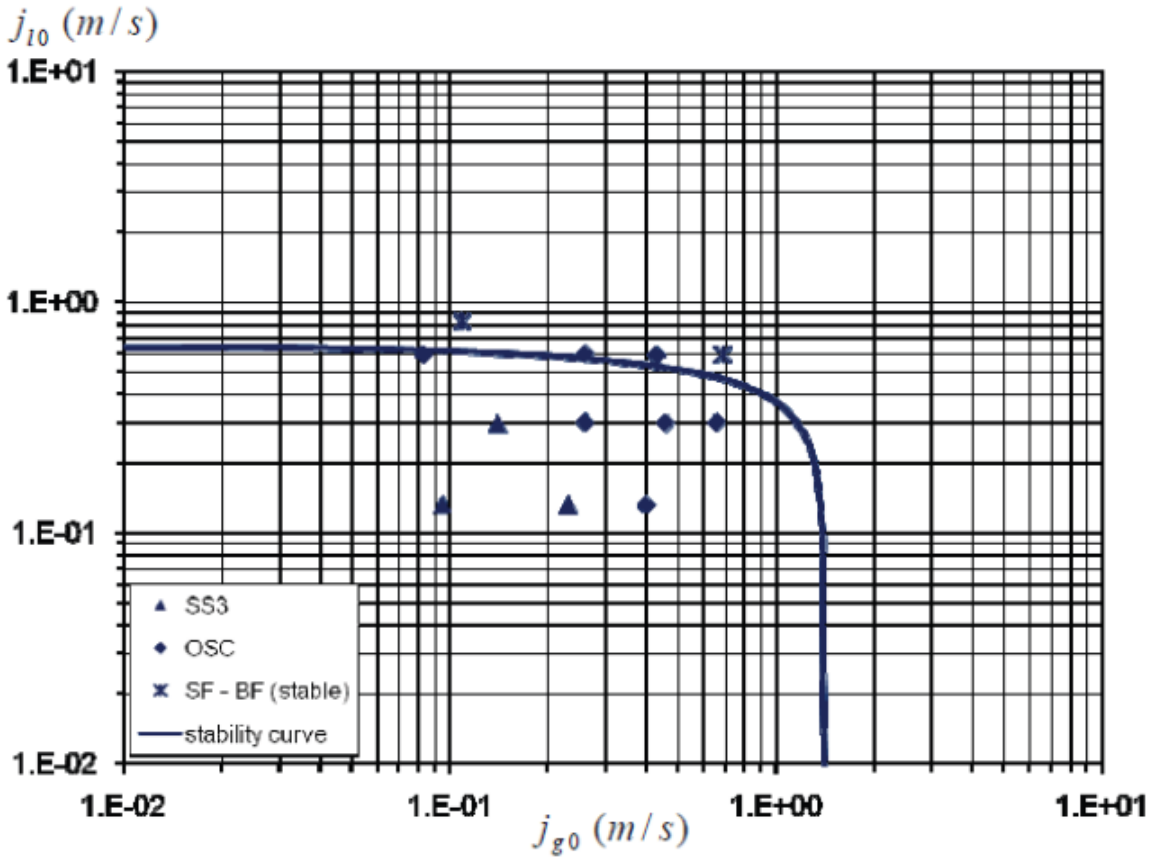

Figure 1.25: Experimental data (Table 1.5) and stability map for $P_s = 4.10\,bara$ and $T = 313\,K$.

Severe slugging flow regime maps

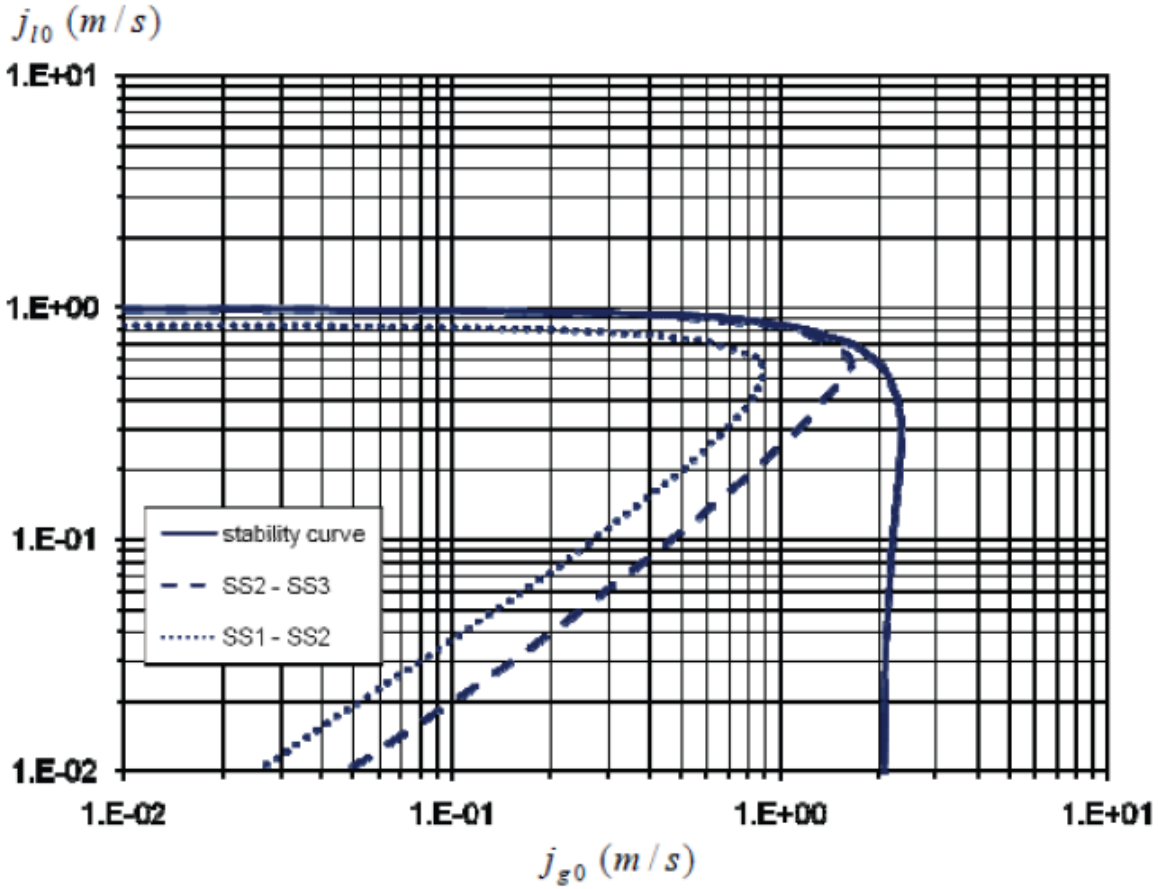

Figure 1.26: Stability and flow regime map for $P_s = 2.013\,bara$ and $T = 293\,K$.

SS flow regime map (Tin, visual)

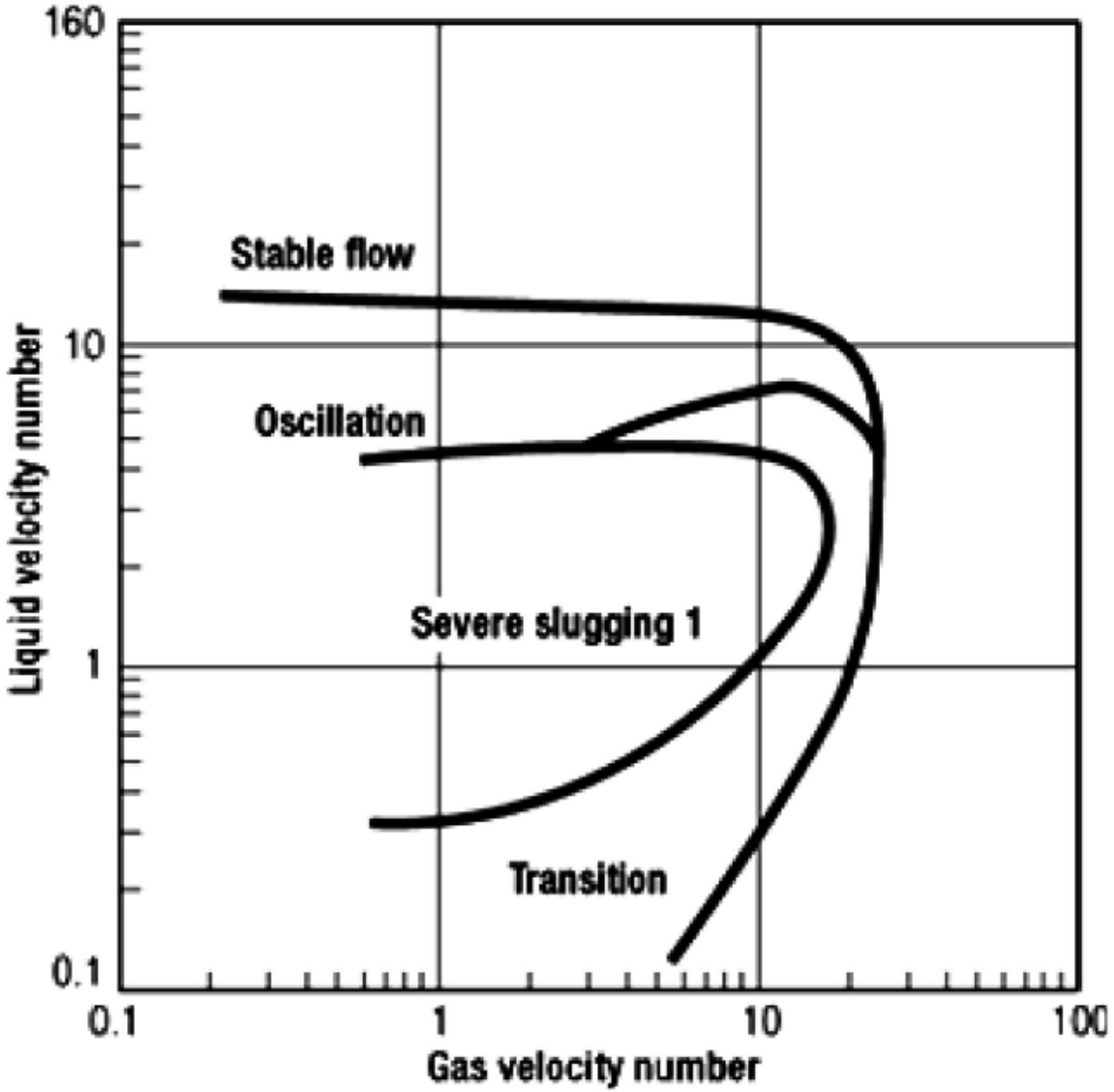

Linear stability analysis

- Although empirical stability criteria (Taitel, 1986; Pots, 1987; Jansen, 1996) are useful for a first estimation of the unstable region (they are even used in commercial steady-state computer codes), a common drawback is that they were not derived from complete dynamic system models, but from ad-hoc conditions in which many physical effects were disregarded; consequently, their applicability is quite limited.
- Linear stability analysis is a more efficient alternative to time domain simulations to identify the stable and unstable regions.
- Other application areas in multiphase flows: flow pattern transitions, boiling crisis, density-wave instabilities.

Linear stability analysis

- Eliminating the void fraction from the algebraic relation, riser equations can be written as:

$$\underline{A_m(v)} + \underline{B_m(v)} \cdot \left\{\frac{\partial v}{\partial t}\right\} + \underline{C_m(v)} \cdot \left\{\frac{\partial v}{\partial s}\right\} = \{0\} \; ; v = \begin{Bmatrix} j_g \\ j_l \\ P \end{Bmatrix} \; ; \; 3 \times 3$$

- Linearization $v(s,t) = \tilde{v}(s) + \hat{v}\,(s,t)$, yields the continuum perturbation equations:

$$\underline{A(\tilde{v})} \cdot \hat{v} + \underline{B(\tilde{v})} \cdot \left\{\frac{\partial \hat{v}}{\partial t}\right\} + \underline{C(\tilde{v})} \cdot \left\{\frac{\partial \hat{v}}{\partial s}\right\} = \{0\}; \quad \hat{v} = \begin{Bmatrix} \hat{j_g} \\ \hat{j_l} \\ \hat{P} \end{Bmatrix} \; ; \; 3 \times 3$$

Linear stability analysis

- Integrating in position and adding the linearized boundary conditions (pipeline equations, choke valve), yields the discretized perturbation problem:

$$\underline{G^*(\tilde{v})} \cdot \left\{\frac{\partial \hat{v}}{\partial t}\right\} + \underline{H^*(\tilde{v})} \cdot \hat{v} = \{0\}; \qquad \hat{v} = \begin{Bmatrix} \underline{\hat{j}_g} \\ \underline{\hat{j}_l} \\ \underline{\hat{P}} \end{Bmatrix} \quad ; \quad 3N \times 3N$$

- System stability depends on the characteristic polynomial:

$$\det\left(\lambda\, \underline{G^*} + \underline{H^*}\right) = 0$$

- $\underline{G^*}$ is singular in NPW model, resulting $2N-2$ finite eigenvalues.

Well posedness

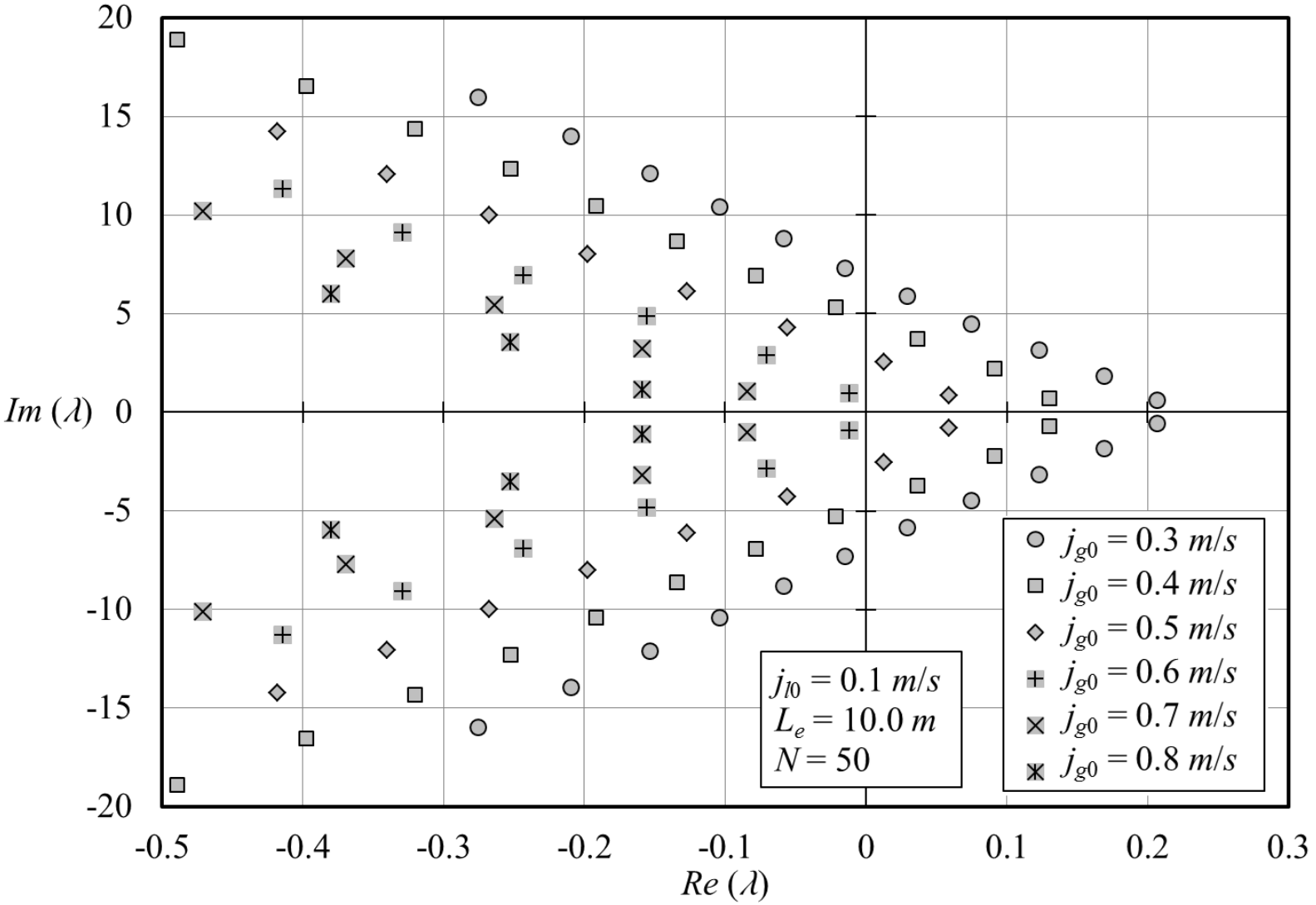

Figure 4: Eigenvalues well-posed behavior in the vicinity of the stability condition, parameters from Taitel et al. (1990).

Nodalization

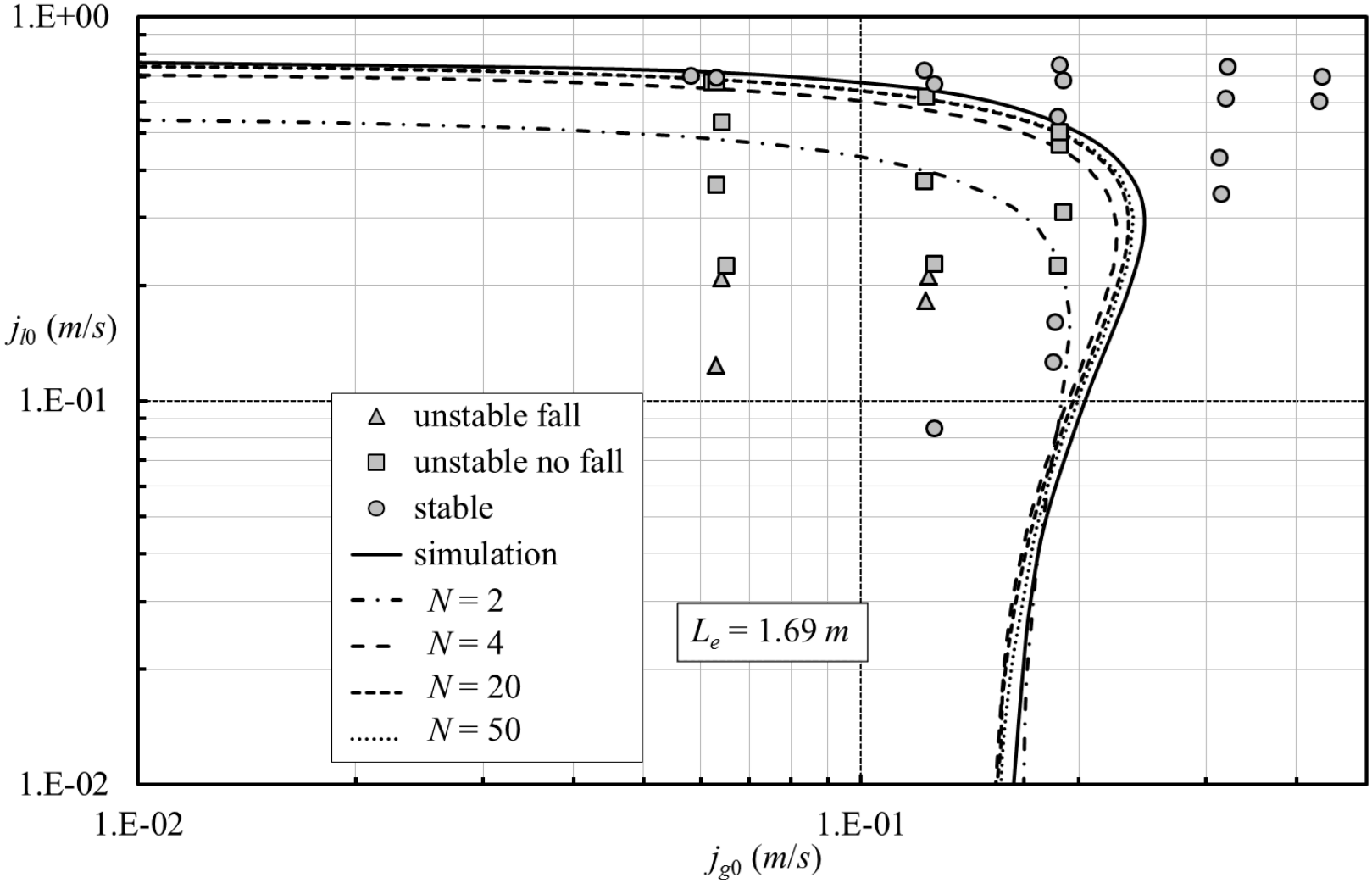

Figure 5: Stability map for a vertical riser with different nodalization, parameters from Taitel et al. (1990).

Parametric study L_e

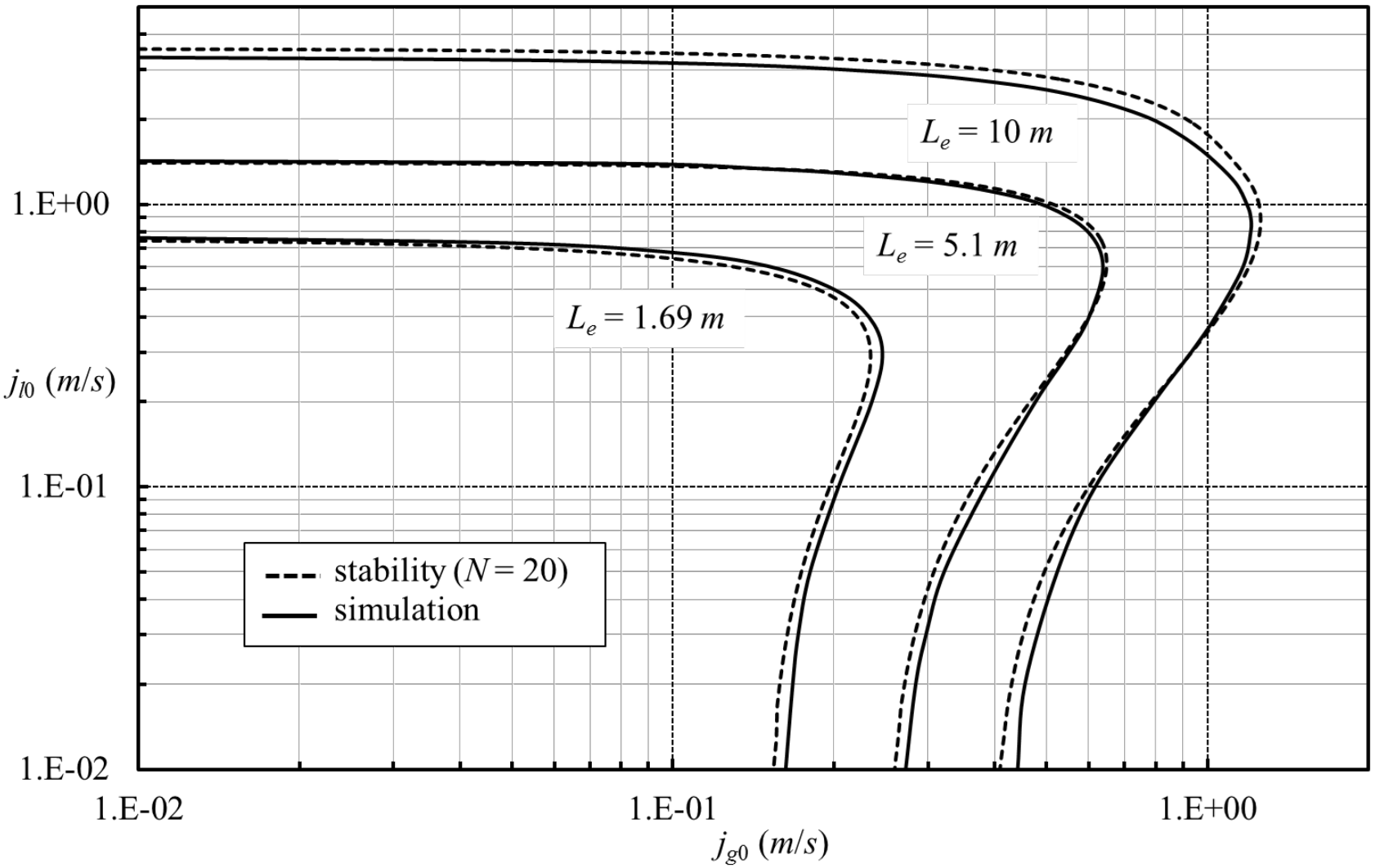

Figure 6: Stability map for a vertical riser with different buffer lengths, parameters from Taitel et al. (1990).

Parametric study $j_{g0\,l}$

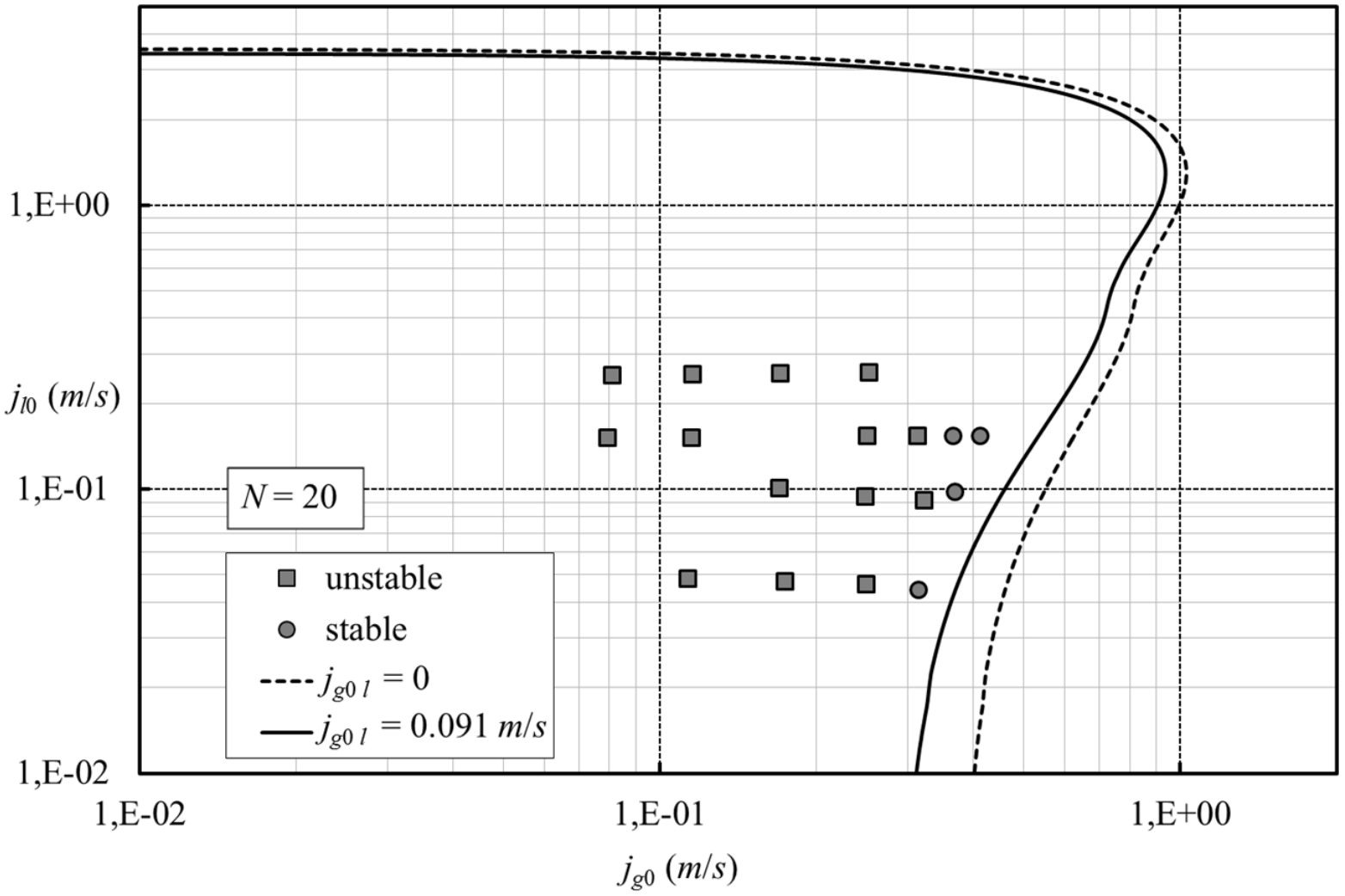

Figure 7: Stability map for a vertical riser with gas injection at the bottom of the riser, parameters from Jansen et al. (1996).

Parametric study K_v

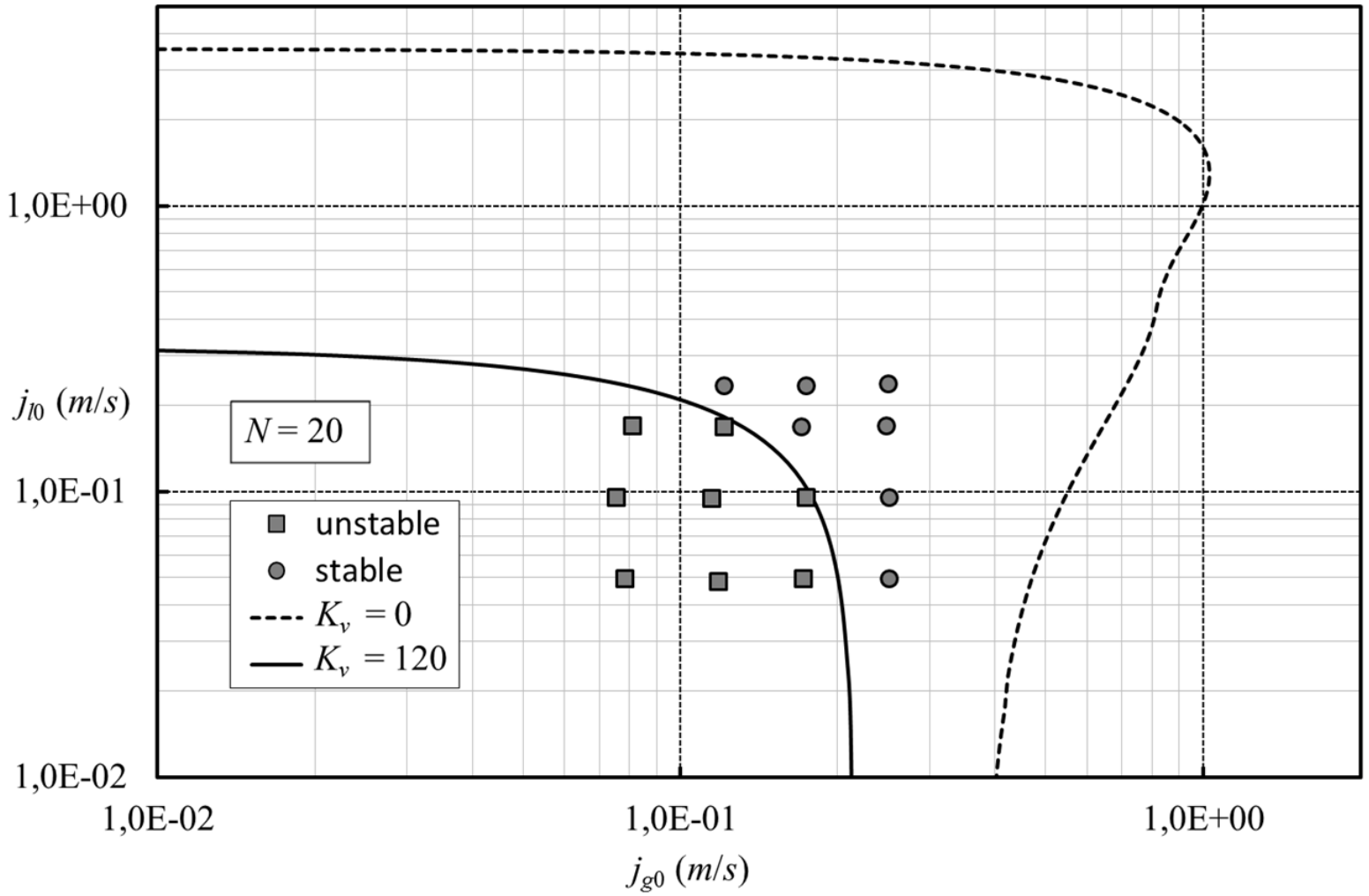

Figure 8: Stability map for a vertical riser with choking at the top of the riser, parameters from Jansen et al. (1996).

Parametric study P_s

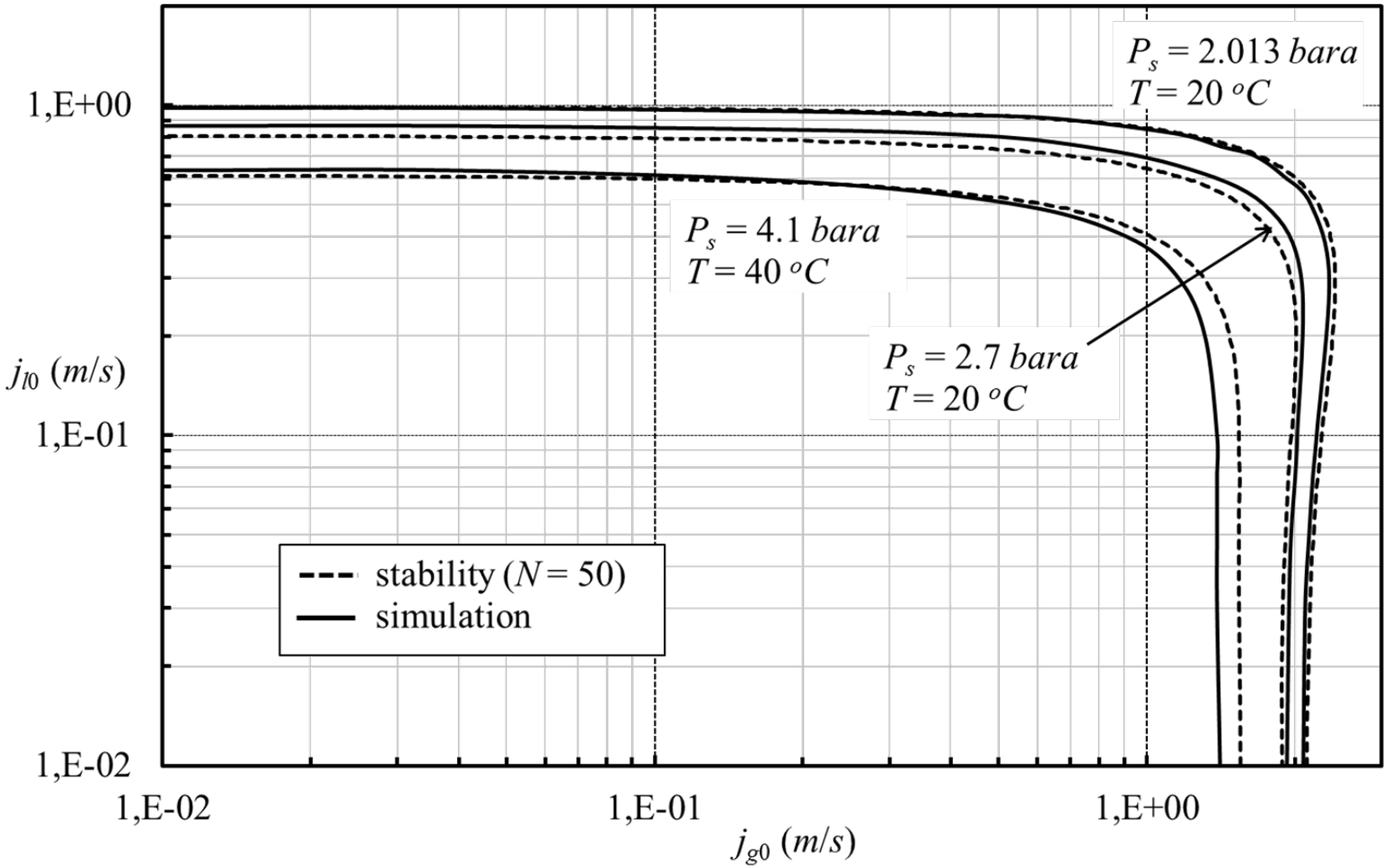

Figure 9: Stability map for a catenary riser for different separation pressures, parameters from Wordsworth et al. (1998).

Publications

Baliño, J. L., Burr, K. P., Nemoto, R. H., Modeling and simulation of severe slugging in air-water pipeline-riser systems, *International Journal of Multiphase Flow* , v.36, p.643 - 660, 2010.

Nemoto, R. H. & Baliño, J. L., Modeling and simulation of severe slugging with mass transfer effects, *International Journal of Multiphase Flow* , v.40, p.144 - 157, 2012.

Baliño, J. L., Modeling and simulation of severe slugging in air-water systems including inertial effects. *Journal of Computational Science* , v.5, p.482 - 495, 2014.

Azevedo, G. R., Baliño, J. L., Burr, K. P., Linear stability analysis for severe slugging in air-water systems considering different mitigation mechanisms, submitted to *International Journal of Multiphase Flow*, 2015

Nemoto, R. H. & Baliño, J. L., The influence of pipeline-riser geometry and produced fluids properties on the occurrence of severe slugging, submitted to *Journal of Petroleum Science and Engineering*.

Papers at JEM 2015

Azevedo, G. R., Baliño, J. L., Burr, K. P., Linear stability analysis for severe slugging including inertial effects.

Yamaguchi, A. J., Baliño, J. L., Experimental study of severe slugging in a air-water pipeline-riser system.

Burr, K. P., Baliño, J. L., Evolution equation for weak hydrodynamic instabilities of two-phase flows in pipeline-riser systems.

Acknowledgements

Petrobras

FAPESP

CNPq

ANP

Thank you!